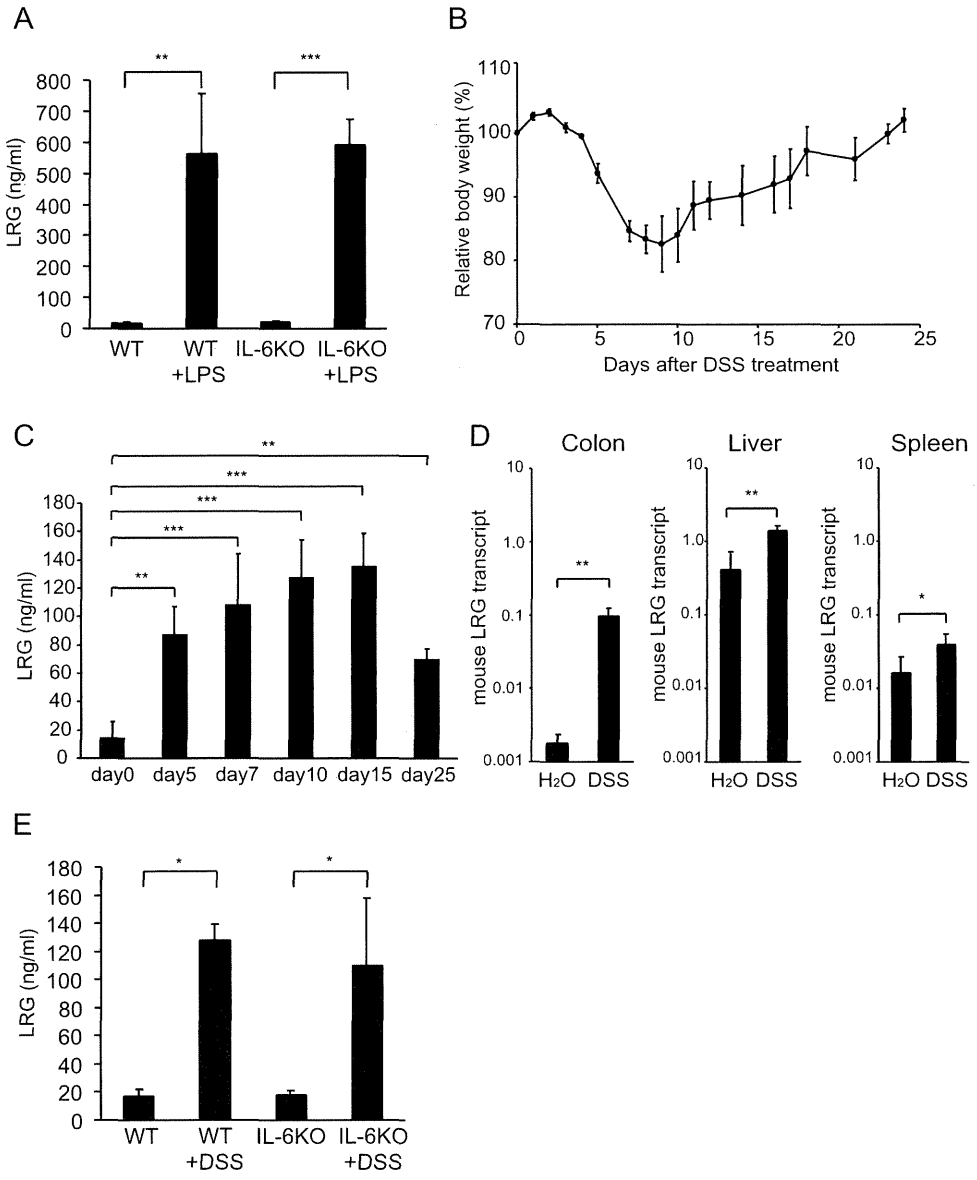

FIGURE 5. Induction of LRG has IL-6-independent pathway in LPS-mediated acute inflammation and active stage of DSS-induced colitis. (A) WT mice and IL-6-deficient mice were injected intraperitoneally with 0 or 10 mg/kg LPS dissolved in 500 μL PBS and serum LRG levels were measured after 24 hours. Data are expressed as mean ± SEM. $^{**}P < 0.005$, $^{***}P < 0.0001$ by one-way ANOVA followed by Scheffe's post-hoc test. (B) Relative body weight changes of mice with DSS-induced colitis in this study. Data are expressed as mean ± SEM ($n = 4$). (C) Expression of LRG is upregulated in murine DSS-induced colitis. At the indicated time, serum LRG levels were determined by ELISA analysis. $^{**}P < 0.005$, $^{***}P < 0.0001$ by one-way ANOVA followed by a by Dunnett's post-hoc test. (D) Nine days after control or DSS treatment, mice were euthanized and gene expression of LRG in the colon, liver, spleen, and kidney was determined by quantitative PCR analysis. Gene expression was calculated relative to HPRT. Data were expressed as mean ± SD ($n = 5$). $^{*}P < 0.05$, $^{**}P < 0.005$ by Student's t-test. (E) IL-6-deficient mice were used for DSS-induced colitis. Nine days after DSS administration, serum levels of mouse LRG was determined by ELISA analysis. $^{*}P < 0.05$ by one-way ANOVA followed by Scheffe's post-hoc test.

however, the strongest induction was observed in colon ($P = 0.000126$).

To investigate whether LRG induction is dependent on IL-6 or not, we analyzed serum LRG levels in IL-6-deficient mice. Interestingly, basal LRG levels in IL-6-deficient mice were similar to those in WT mice and LRG was robustly induced by LPS administration in IL-6-deficient mice (Fig. 5A). Moreover, increased serum LRG levels were also detected in the active stage (day 9) of DSS-induced colitis in IL-6-deficient mice (Fig. 5E). Importantly, the increase of serum LRG in IL-6-deficient mice was similar to that in WT mice (Fig. 5A,E). These findings indicate that LRG expression can be induced in the absence of IL-6.

DISCUSSION

In this study we first demonstrated that serum LRG levels were significantly increased in sera of active UC patients compared with patients in remission and HC. Serum LRG is likely elevated in diverse racial groups, because we detected increased serum LRG levels not only in Japanese patients (Fig. 1A)[13] but also in Caucasian patients with UC (Fig. 1C,D) and CD (data not shown). In addition, levels of serum LRG were significantly correlated with disease activity in UC and the correlation was stronger than CRP. Moreover, by analyzing ROC curve and AUC, serum LRG levels showed higher AUC than CRP and serum LRG levels represented superior sensitivity and specificity to CRP for remission and active of UC by CAI (Fig. 2D), indicating that LRG is a useful marker to evaluate disease activity in UC. In the normal state, serum LRG is thought to be produced from liver and LRG is abundantly found in the sera of HC. In colonic inflammation, we found that the expression of LRG is increased in the inflamed mucosa of UC patients and mice with DSS colitis, suggesting that inflamed tissues can be a source for production of LRG (Fig. 3). The increased expression of LRG in inflamed tissue has previously been observed in appendix during acute appendicitis.[28] Moreover, in acute inflammatory disorders, including appendicitis and diverticulitis, increased expression of serum LRG was observed (Fig. 1A). These results indicate that the elevated expression of LRG at inflamed sites and in sera occurs in various acute and chronic inflammatory disorders. Therefore, increased serum LRG levels are not suitable for use as a specific diagnostic marker of IBD.

CRP is the most common serum marker used to evaluate disease activity in inflammatory diseases. However, serum CRP is primarily dependent on liver production induced by circulating IL-6. Compared with CD and RA, only modest to absent CRP responses are observed in UC, despite active inflammation in colon.[9] Indeed, our cohort of 82 UC patients, analyzed in this study, included five patients with normal value of CRP while having active disease (Fig. 2A). However, our study demonstrated that serum LRG levels were significantly increased in active UC patients' sera and correlated better with disease activity of UC than CRP levels (Figs. 1A, 2A). Particularly, in the group of patients with negative CRP (CRP <0.2), significant correlation was observed between serum LRG levels and CAI (Supporting Fig. 2C). Similarly, among CRP-negative patients serum LRG levels were significantly elevated in those with endoscopically active UC, compared with UC in remission (Supporting Fig. 1B). In addition, serum LRG levels were decreased after therapy (Fig. 2C), suggesting that LRG is a useful serological biomarker for evaluating disease activity and therapeutic effect in UC.

Better correlation of serum LRG levels with disease activity of UC than CRP might be explained in part by the differences in induction mechanisms between LRG and CRP. While the expression of CRP is essentially dependent on IL-6, several cytokines may compensate for the absence of elevated IL-6 in induction of LRG expression. Accordingly, expression of LRG in COLO205 cells was induced not only by IL-6 but also by TNF-α and IL-22 (Fig. 4B), all of which were increased in sera of UC patients (Fig. 4A). Expression of LRG was strongly induced by IL-22 in COLO205 cells, correlating with enhanced STAT3 (Tyr705) phosphorylation by IL-22 compared with IL-6 (data not shown). Thus, inflammatory cytokines such as TNF-α and IL-22 may mediate LRG expression in the absence of IL-6. Moreover, using DSS-induced colitis in IL-6-deficient mice we could demonstrate an IL-6-independent pathway for LRG induction (Fig. 5E). Because promoter regions of human and mouse LRG share high sequence homology and contain putative binding sites for transcription factors such as C/EBP, MZF1, and STAT,[17] it is conceivable that the similar IL-6-independent mechanisms of LRG induction are also involved in humans. Future studies are required to fully elucidate the induction mechanisms of LRG in both humans and mice.

In the three disease categories of UC based on extent of disease, serum LRG levels tended to be low in proctitis compared with extensive colitis and left-sided colitis (Fig. 1B). In addition, correlation between serum LRG levels and disease activity did not reach significance in proctitis (Fig. 2B). Although the low number of patients with active proctitis may preclude the proper evaluation of LRG levels, limited inflamed area of proctitis may also be a reason for slight increases of serum LRG levels in these patients. Given the increased production of LRG in inflamed colonic mucosa, fecal LRG might be a more sensitive disease biomarker for UC including proctitis. Optimization for the measurement of fecal LRG is currently under way in our laboratory.

This study also highlights the potential usefulness of LRG in evaluating murine colitis. Our results indicate that serum LRG levels increase as the disease progresses in a DSS-induced colitis model (Fig. 5B,C). In addition, the LRG expression is significantly upregulated in the colon with DSS-induced colitis (Fig. 5D). Thus, LRG in mice can be an objective disease activity marker for colitis models and may be useful for preclinical studies of IBD.

In conclusion, serum LRG levels reflect disease activity of UC better than CRP, especially in patients with low CRP. In the inflammatory condition, LRG is expressed in the inflamed tissue and expression of LRG is regulated by mechanisms different from that of CRP. These findings suggest that serum LRG is a novel and potential serologic biomarker for evaluating disease activity of UC.

ACKNOWLEDGMENTS

We thank T. Mizushima for provision of appendicitis and diverticulitis patients' sera, Y. Kanazawa for secretarial

assistance, and M. Urase and A. Morimoto for technical assistance.

REFERENCES

1. Nikolaus S, Schreiber S. Diagnostics of inflammatory bowel disease. *Gastroenterology*. 2007;133:1670–1689.
2. Baumgart DC, Sandborn WJ. Inflammatory bowel disease: clinical aspects and established and evolving therapies. *Lancet*. 2007;369: 1641–1657.
3. Stange EF, Travis SP, Vermeire S, et al. European evidence based consensus on the diagnosis and management of Crohn's disease: definitions and diagnosis. *Gut*. 2006;55(Suppl 1):i1–15.
4. Caprilli R, Viscido A, Latella G. Current management of severe ulcerative colitis. *Nat Clin Pract Gastroenterol Hepatol*. 2007;4:92–101.
5. Kornbluth A, Sachar DB. Ulcerative colitis practice guidelines in adults (update): American College of Gastroenterology, Practice Parameters Committee. *Am J Gastroenterol*. 2004;99:1371–1385.
6. Sands BE, Abreu MT, Ferry GD, et al. Design issues and outcomes in IBD clinical trials. *Inflamm Bowel Dis*. 2005;11(Suppl 1):S22–28.
7. Freeman HJ. Use of the Crohn's disease activity index in clinical trials of biological agents. *World J Gastroenterol*. 2008;14:4127–4130.
8. Best WR, Becktel JM, Singleton JW, et al. Development of a Crohn's disease activity index. National Cooperative Crohn's Disease Study. *Gastroenterology*. 1976;70:439–444.
9. Vermeire S, Van Assche G, Rutgeerts P. C-reactive protein as a marker for inflammatory bowel disease. *Inflamm Bowel Dis*. 2004;10: 661–665.
10. Pepys MB, Druguet M, Klass HJ, et al. Immunological studies in inflammatory bowel disease. *Ciba Found Symp* 1977:283–304.
11. Saverymuttu SH, Hodgson HJ, Chadwick VS, et al. Differing acute phase responses in Crohn's disease and ulcerative colitis. *Gut*. 1986; 27:809–813.
12. Colombel JF, Rutgeerts P, Reinisch W, et al. Early mucosal healing with infliximab is associated with improved long-term clinical outcomes in ulcerative colitis. *Gastroenterology*. 2011;141:1194–1201.
13. Serada S, Fujimoto M, Ogata A, et al. iTRAQ-based proteomic identification of leucine-rich alpha-2 glycoprotein as a novel inflammatory biomarker in autoimmune diseases. *Ann Rheum Dis*. 2010;69:770–774.
14. Haupt H, Baudner S. Isolation and characterization of an unknown, leucine-rich 3.1-S-alpha2-glycoprotein from human serum [author's transl]. *Hoppe Seylers Z Physiol Chem*. 1977;358:639–646.
15. Takahashi N, Takahashi Y, Putnam FW. Periodicity of leucine and tandem repetition of a 24-amino acid segment in the primary structure of leucine-rich alpha 2-glycoprotein of human serum. *Proc Natl Acad Sci U S A*. 1985;82:1906–1910.
16. Shirai R, Hirano F, Ohkura N, et al. Up-regulation of the expression of leucine-rich alpha(2)-glycoprotein in hepatocytes by the mediators of acute-phase response. *Biochem Biophys Res Commun*. 2009;382: 776–769.
17. O'Donnell LC, Druhan LJ, Avalos BR. Molecular characterization and expression analysis of leucine-rich alpha2-glycoprotein, a novel marker of granulocytic differentiation. *J Leukoc Biol*. 2002;72: 478–485.
18. Rachmilewitz D. Coated mesalazine (5-aminosalicylic acid) versus sulphasalazine in the treatment of active ulcerative colitis: a randomised trial. *BMJ*. 1989;298:82–86.
19. Kruis W, Schreiber S, Theuer D, et al. Low dose balsalazide (1.5 g twice daily) and mesalazine (0.5 g three times daily) maintained remission of ulcerative colitis but high dose balsalazide (3.0 g twice daily) was superior in preventing relapses. *Gut*. 2001;49:783–789.
20. Matts SG. The value of rectal biopsy in the diagnosis of ulcerative colitis. *Q J Med*. 1961;30:393–407.
21. Iwahori K, Serada S, Fujimoto M, et al. Overexpression of SOCS3 exhibits preclinical antitumor activity against malignant pleural mesothelioma. *Int J Cancer*. 2011;129:1005–1017.
22. Kim A, Enomoto T, Serada S, et al. Enhanced expression of Annexin A4 in clear cell carcinoma of the ovary and its association with chemoresistance to carboplatin. *Int J Cancer*. 2009;125:2316–2322.
23. Fujimoto M, Nakano M, Terabe F, et al. The influence of excessive IL-6 production in vivo on the development and function of Foxp3+ regulatory T cells. *J Immunol*. 2011;186:32–40.
24. Murch SH, Lamkin VA, Savage MO, et al. Serum concentrations of tumour necrosis factor alpha in childhood chronic inflammatory bowel disease. *Gut*. 1991;32:913–917.
25. Woywodt A, Ludwig D, Neustock P, et al. Mucosal cytokine expression, cellular markers and adhesion molecules in inflammatory bowel disease. *Eur J Gastroenterol Hepatol*. 1999;11:267–276.
26. Andoh A, Zhang Z, Inatomi O, et al. Interleukin-22, a member of the IL-10 subfamily, induces inflammatory responses in colonic subepithelial myofibroblasts. *Gastroenterology*. 2005;129:969–984.
27. Okayasu I, Hatakeyama S, Yamada M, et al. A novel method in the induction of reliable experimental acute and chronic ulcerative colitis in mice. *Gastroenterology*. 1990;98:694–702.
28. Kentsis A, Lin YY, Kurek K, et al. Discovery and validation of urine markers of acute pediatric appendicitis using high-accuracy mass spectrometry. *Ann Emerg Med*. 2010;55:62–70 e4.

Tumor Biol. (2012) 33:1141–1149
DOI 10.1007/s13277-012-0356-9

RESEARCH ARTICLE

Serum HE4 as a diagnostic and prognostic marker for lung cancer

Kota Iwahori · Hidekazu Suzuki · Yoshiro Kishi · Yoshihiro Fujii · Rie Uehara · Norio Okamoto · Masashi Kobayashi · Tomonori Hirashima · Ichiro Kawase · Tetsuji Naka

Received: 19 December 2011 / Accepted: 9 February 2012 / Published online: 29 February 2012

Abstract We evaluated the diagnostic and prognostic efficacy of human epididymis protein 4 (HE4) for lung cancer patients by using our novel enzyme-linked immunosorbent assay (ELISA) system. We measured serum HE4 levels of cancer patients including 49 lung cancer and 18 ovarian cancer patients. Furthermore, we evaluated the relationship between serum HE4 levels and overall survival after chemotherapy of 24 lung cancer patients. Serum HE4 levels were significantly higher for non-small, small cell lung cancer and ovarian cancer patients than for healthy controls. The area under the receiver operating characteristic curve (AUC) was calculated for differentiation of lung cancer patients and healthy controls. AUC for serum HE4 was 0.988 for differentiating lung cancer patients from healthy controls, with a cutoff value of 6.56 ng/ml (sensitivity= 89.8%, specificity=100%). Serum HE4 levels were elevated in 36/40 (90.0%) non-small cell lung cancer patients, 8/9 (88.9%) small cell lung cancer patients and 8/18 (44.4%) ovarian cancer patients. High levels of serum HE4 (>15 ng/ml) after chemotherapy were significantly correlated with worse overall survival after the treatment. These findings suggest that serum HE4 is a potential diagnostic and prognostic marker for lung cancer patients.

Keywords HE4 · Tumor marker · ELISA · Lung cancer · Chemotherapy

K. Iwahori · T. Naka (✉)
Laboratory for Immune Signal,
National Institute of Biomedical Innovation,
7-6-8 Saito-Asagi,
Ibaraki, Osaka 567-0085, Japan
e-mail: tnaka@nibio.go.jp

K. Iwahori
Department of Respiratory Medicine, Allergy, and Rheumatic Diseases, Osaka University Graduate School of Medicine,
2-2 Yamada-oka,
Suita, Osaka 565-0871, Japan

H. Suzuki · N. Okamoto · M. Kobayashi · T. Hirashima · I. Kawase
Department of Thoracic Malignancy, Osaka Prefectural Medical Center for Respiratory and Allergic Diseases,
3-7-1 Habikino,
Habikino, Osaka 583-8588, Japan

Y. Kishi · Y. Fujii · R. Uehara
Medical & Biological Laboratories, Co., Ltd.,
4-5-3, Sakae, Naka-ku,
Nagoya 460-0008, Japan

Introduction

Lung cancer is the leading cause of death in adult men in Europe, the United States, and Japan. In 2010, approximately 157,300 Americans died of lung cancer from among 569,490 cancer deaths [1]. The exceptionally high mortality rate of lung cancer is, in part, due to the fact that lung cancer is often diagnosed at a late stage when the prognosis is usually poor, and early detection continues to be an elusive goal. For patients with advanced stage disease, modest but real improvements in overall survival and quality of life have been achieved with systemic chemotherapy [2]. However, the determination of efficacy of chemotherapy during the early phase of treatment is difficult to achieve. The decision whether to continue or to stop chemotherapy is traditionally guided by imaging-based tumor response evaluation, which is regarded as a surrogate marker of clinical benefit. Assessment by structural imaging has known limitations and also may have a poor correlation with pathologic response in non-small cell lung cancer [3]. On the other

hand, tumor markers that are currently available for lung cancer such as carcinoembryonic antigen (CEA), serum cytokeratin 19 fragment (CYFRA 21-1) and progastrin-releasing peptide (pro-GRP) are not satisfactory for diagnosis at an early stage or for monitoring the disease because of their relatively low sensitivity and specificity in detecting the presence of cancer cells [4–6]. Therefore, the identification of novel diagnostic and prognostic biomarkers for treatment response is eagerly desired.

Human epididymis protein 4 (HE4) was first identified in the epithelium of the distal epididymis and originally predicted to be a protease inhibitor involved in sperm maturation [7, 8]. Regarding malignant neoplasms, gene expression profiling studies have identified upregulation of HE4 in ovarian cancer [9–14], and several studies have shown HE4 protein expression in ovarian cancer, providing the opportunity for its application in histopathologic diagnosis [15–18]. Recent studies have revealed elevated HE4 protein levels in serum from ovarian cancer patients [19]. Moreover, HE4 protein expression was analyzed in other neoplasms including lung cancer [20, 21]. In this study, we developed novel enzyme-linked immunosorbent assay (ELISA) system to detect serum HE4, and by using this system, we showed that HE4 has potential for diagnostic marker of lung cancer. Specifically, we found that HE4 level after chemotherapy is strongly correlated with survival after the treatment.

Materials and methods

Patients and controls for measurement of HE4

Serum samples were collected from 49 consecutive patients with lung cancer (33 with adenocarcinoma, six with squamous cell carcinoma, one with large cell carcinoma and nine with small cell carcinoma), 18 with ovarian cancer, 10 with gastric cancer and eight with colon cancer. For control, we used 37 healthy adults (Table 1). The age range in 37 healthy control subjects was between 24 and 65 years. The age range in 49 lung cancer patients was between 40 and 78 years. We obtained written and oral informed consent from all participants. This study was approved by our institutional review board (IRB).

Patients for evaluation of chemotherapy

This prospective, IRB-approved study included 24 patients enrolled between 28 April 2008 and 26 August 2008. Patient characteristics are presented in Table 2. The median age was 69 years (45–76 years). All patients received chemotherapies. Specific regimens are presented in Table 2. Computed tomography (CT) scans were performed after 2 cycles of chemotherapy or 1 month of gefitinib/erlotnib therapy. All patients had measurable disease. Response categories were defined according to the Response Evaluation Criteria in Solid Tumors (RECIST) as complete response (CR), partial response (PR), stable disease (SD) and progressive disease (PD).

Cell lines

Nonsmall cell lung cancer cell lines A549, NCI-H1793, LU61, PC14, PC14PE6, PC9, SKLU1 and SKMES2; breast cancer cell line MCF7; colon cancer cell lines LOVO and WiDr; gastric cancer cell lines GC1Y, GT3TKB, HGC27, KATO3, MKN45 and OCUM1; pancreatic cancer cell line Miapaca2; prostate cancer cell lines 22Rv1 and PC3; and bladder cancer cell line T24 were cultured in DMEM medium (Sigma, St Louis, MO) supplemented with 10% fetal bovine serum (Equitech Bio Inc., Kerrville, TX). Non-small cell lung cancer cell line A427 was cultured in E-MEM medium (Sigma) supplemented with 10% fetal bovine serum. Non-small cell lung cancer cell lines NCI-H226, NCI-H358, NCI-H520, NCI-H522, NCI-H596, NCI-H2170, LC174, LC319 and ChagoK1; small cell lung cancer cell line DMS114; gastric cancer cell lines SCH, MKN74 and MKN1; pancreatic cancer cell lines KLM1, PK59 and PK1; and breast cancer cell line T47D were cultured in RPMI (Sigma) supplemented with 10% fetal bovine serum.

Table 1 Serum concentrations of HE4 in cancer patients and controls

Diagnosis	Number of study participants	HE4 (ng/ml)			Positive ratio (%)
		Mean (SD)	Median	Range	(Cutoff 6.56 ng/ml)
Lung cancer	49	14.0 (9.5)	11.4	4.3–63.4	89.8
NSCLC	40	13.3 (6.5)	11.4	4.3–30.7	90.0
SCLC	9	17.3 (18.1)	11.4	5.5–63.4	88.9
Ovarian cancer	18	10.9 (13.6)	6.1	2.0–60.2	44.4
Gastric cancer	10	7.2 (4.4)	7.1	2.1–17.4	60.0
Colorectal cancer	8	7.7 (3.5)	7.1	3.0–12.2	62.5
Normal	37	2.7 (1.2)	2.4	1.3–5.8	

Table 2 Patient characteristics

Characteristics	Number of patients
Gender	
Males/females	16/8
Age (years)	
<71/>71	13/11
Stage	
3A/3B/4	4/5/15
Tumor histology	
Adenocarcinoma	15
Squamous	4
Unclassified NSCLC	1
Small	4
Chemotherapy	
NSCLC	
Carboplatin + paclitaxel	5
Vinorelbine	3
Irinotecan	3
Cisplatin + gemcitabine	2
Gefitinib	2
Erlotinib	2
Carboplatin + gemcitabine	1
Cisplatin + vinorelbine	1
Gemcitabine	1
SCLC	
Carboplatin + etoposide	2
Cisplatin + etoposide	1
Cisplatin + irinotecan	1
Clinical response	
NSCLC	
CR/PR/SD/PD	0/5/10/5
SCLC	
CR/PR/SD/PD	0/3/1/0

Culture supernatants were collected at 5 to 6 days after cultivation and stored at 4°C until test.

Antigen preparation

Recombinant human HE4 protein was produced by amplifying the part coding for amino acids 1–124 from the cDNA encoding the transcript for human HE4 (Genbank accession no. NM_006103) with DNA polymerase (recombinant Taq polymerase; Takara Bio Inc., Shiga, Japan) and using the primers 5′-CGGGATCCGAGAAGACTGGCGTGTGCCCCG-3′ and 5′-TTTAAAGCGGCCGCTCAGAAATTGGGAGTGACA CAGG-3′. The amplified DNA was inserted into the *Bam*HI/*Not*I site of a mammalian expression plasmid DNA vector pSecTag2/Myc-His (Invitrogen, Carlsbad, CA) and transfected into HEK 293 T cells by lipofection (Lipofectamine 2000; Invitrogen). The culture supernatant of the transfectant was recovered at 5 days after lipofection and applied to a TALON resin to purify the secreted His-tagged proteins according to the manufacturer's instructions (Takara). The purified HE4 protein thus obtained was dialyzed with 4.0 l of PBS twice and kept frozen at −80°C until use as an immunogen or as a standard polypeptide for sandwich ELISA. Purity of the recombinant HE4 was confirmed by Coomassie Brilliant Blue (CBB) staining after electrophoresis under reduced condition (Fig. 1a).

Membrane-bound form of HE4 was constructed by molecular fusion together with the transmembrane region of a type I cell surface protein HIDE1 (accession number: A8MVS5) as briefly described below. Membrane-bound form of HE4 was produced by amplifying the part coding for amino acids 1–125 and 114–164 from the cDNAs of HE4 gene and HIDE1 gene, respectively, and both amplified DNAs were inserted into the *Xba*I site of pcDNA3.1/myc-His. *IRES-GFP* gene (Cell Biolabs, Inc., San Diego, CA) was then inserted into the *Pme*I site of the same plasmid DNA. The plasmid DNA was transfected into HEK 293 T cells, and GFP-positive cells were accounted for the cells expressing membrane bounded HE4.

Immunogen to develop a polyclonal antibody to human HE4 was prepared as follows. The part coding for amino acids 31–124 of the HE4 cDNA was ligated to the *Eco*RI/*Xho*I site of a bacterial expression vector pET28a (Novagen, Madison, WI). BL21 (DE3) competent cell (Takara) was transformed with the pET28a plasmid and cultured in LB medium. After induction of expression of HE4 protein using IPTG, the bacteria was collected and lysed with PBS containing 8 M urea, 1% NP-40, 0.5 mM PMSF and protease inhibitor cocktail (Sigma, St. Louis, MO). After centrifugation at 13,000*g* for 15 min, the supernatant containing His-tagged HE4 protein was loaded on a TALON resin, and the recombinant HE4 was eluted from the resin with 200 mM imidazole solution according to the manufacturer's instructions (Takara).

Antibody generation

To generate monoclonal antibodies against human HE4, 4-week-old BALB/c mice were immunized intraperitoneally with the recombinant HE4 produced from 293 T transfectant on days 0, 7, 14 and 16 (10 μg/shot). Following the last immunization, lymphocytes of the spleen were collected and fused with P3U1 myeloma cells in a 50% polyethylene glycol 4000 solution (Wako, Osaka, Japan) on day 18. The fused cells were plated on 96-well plates with RPMI-1640 medium containing 15% fetal calf serum (Equitech-Bio), penicillin/streptomycin (Invitrogen, Carlsbad, CA) and HAT solution (Invitrogen). After 10 days of incubation at 37°C with 5% CO_2 in a humidified environment, culture supernatants were collected and screened for their ability to bind to the immunogen by ELISA using recombinant HE4. Selected positive hybridoma colonies were expanded and

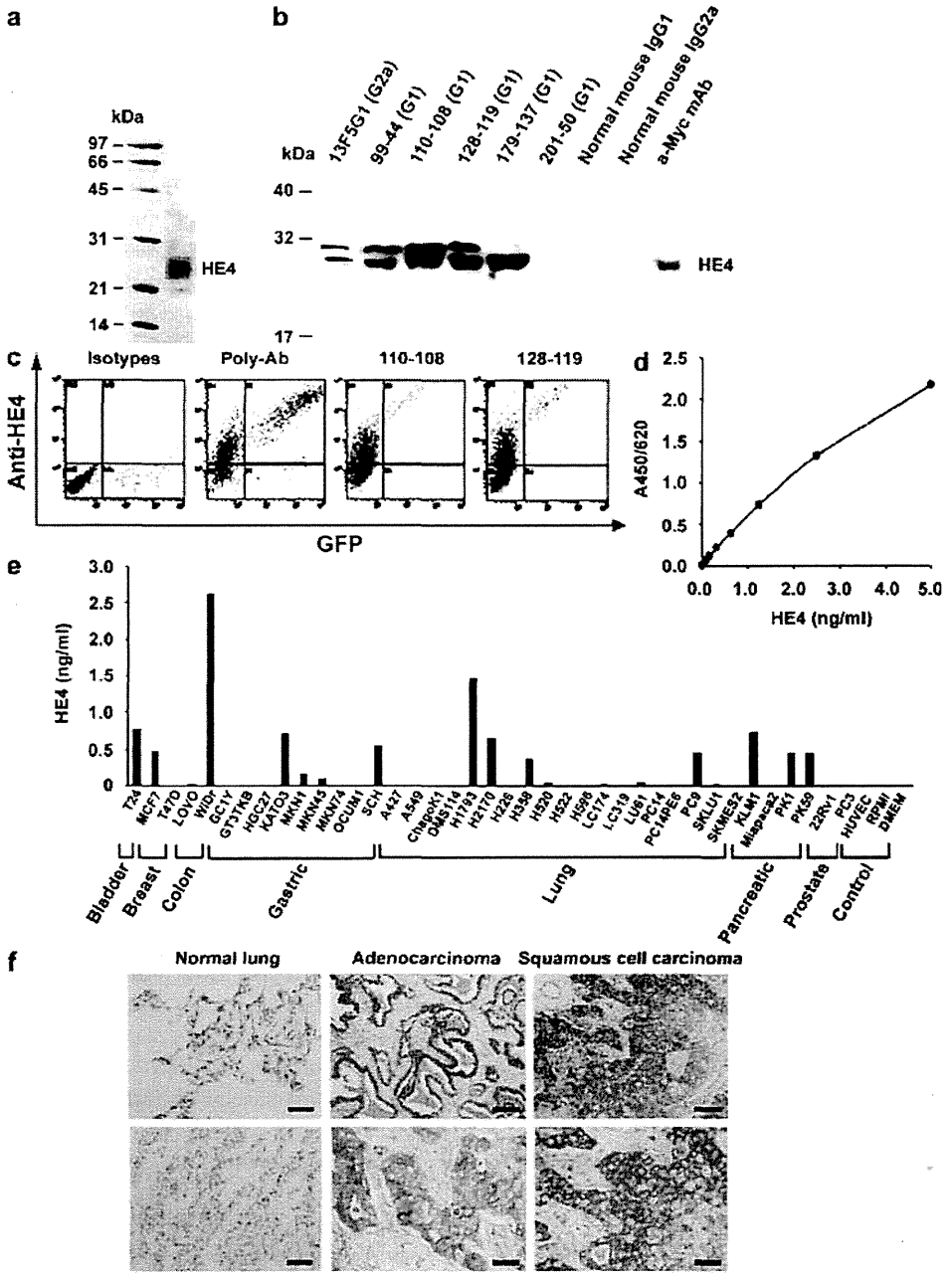

Fig. 1 **a** Purity of the prepared recombinant HE4 proteins for immunization. Proteins were electrophoresed under reduced condition and stained with Coomassie Brilliant Blue. **b** Reactivity of anti-HE4 antibodies to recombinant HE4 protein. Anti-HE4 antibodies were used for immunoprecipitation. Recovered proteins were separated by SDS-PAGE and electrotransferred to polyvinylidenefluoride (PVDF) membranes. Membranes were probed with anti-myc antibody for myc-His tagged HE4. Recombinant HE4 protein was applied for positive control. **c** Expression of HE4 on the surface of HE4-transfected 293 T cells. 293 T cells were incubated with anti-HE4 antibodies (110-108 and 128-119) or an isotype-matched control antibody and followed by PE-conjugate anti mouse IgG. Antigen expression was detected by flow cytometry. **d** Standard curves for HE4 in sandwich ELISA. ELISA displaying the mean absorbance values from indicated concentrations of recombinant proteins. **e** HE4 levels in the supernatants of cell lines measured by specific ELISA systems. **f** Immunohistochemical analysis of HE4 in lung cancer tissue. *Scale bar upper panels* 100 μm, *scale bar lower panels* 50 μm

subcloned by limiting dilution. An isostrip kit (Hoffmann-La Roche, Basel, Switzerland) was used for antibody isotype determination according to the manufacturer's instructions. Antibody purification was carried out with protein A affinity chromatography (GE Healthcare, Buckinghamshire, UK). Following a competition assay for the immunogen among the clones thus obtained (data not shown), clone 110-108 (IgG1) and clone 128-119 (IgG1) were selected to construct a sandwich ELISA for the detection of HE4.

Polyclonal antibody to recombinant human HE4 was prepared by injecting Japanese white rabbits (Kitayama Labs, Nagano, Japan) with purified HE4 (100 μg/injection) from *E. coli* subcutaneously in complete Freund's adjuvant followed by subsequent boosts in incomplete Freund's (Sigma). The serum was collected and IgG-purified with Protein G Sepharose (GE Healthcare).

Flow cytometry

At 24 h after transfection of the plasmid DNA-encoding membrane-binding HE4 into 293 T cells, the transfectant was treated with PBS containing 5 mM EDTA for 3 min to

detach from the culture dish, washed with PBS twice and incubated with 1 μg/ml of anti-HE4 antibodies or isotype-matched control for 30 min at 4°C in PBS containing 0.5% BSA and 2 mM EDTA. Following washing with the above buffer twice, PE conjugate antimouse IgG (MBL, Nagoya, Japan) for monoclonal antibody and PE-conjugated anti-rabbit polyclonal antibody (MBL) were added and further incubated for 30 min at 4°C. All flow cytometry was performed on Cytomics FC500 (Beckman Coulter, Fullerton, CA).

Immunoprecipitation and Western blot

The reactivity of anti-HE4 antibodies to recombinant HE4 protein was confirmed by immunoprecipitation. Fifteen microliters of Protein G sepharose suspended in PBS containing 0.01% BSA (Sigma) was incubated with 5 μg of anti-HE4 antibodies for 2 h at 4°C with gentle rocking. During this step, 250 ng of the recombinant myc-His-tagged HE4 protein was incubated with Protein G beads for 30 min at 4°C with shaking to preclear the samples. The Protein G Sepharose incubated with the antibodies were centrifuged at 1,000*g* for 2 min and washed with PBS three times. Then, the precleared samples were added to the tube containing the washed Protein G sepharose and rotated overnight at 4°C. After the incubation, the beads were washed with PBS three times and boiled in 25 μl of 2× Laemmli's SDS sample buffer for 5 min. Proteins (20 μl of sample per lane) were separated by sodium dodecylsulfate-polyacrylamide gel electrophoresis (SDS-PAGE) on a 12.5% polyacrylamide gel and electrotransfered to a polyvinylidenefluoride (PVDF) membrane. The membrane blocked with 5% nonfat milk in PBS containing 0.05% Tween 20 (blocking buffer) was incubated with 1.0 μg/ml mouse monoclonal anti-Myc antibody (MBL) to react with the precipitated Myc-His-tagged HE4 for 1 h at room temperature. After three washes with PBS containing 0.05% Tween 20, the membrane was incubated with a horseradish peroxidase (HRP)-conjugated antimouse IgG (MBL) diluted 1:5,000 with the blocking buffer. Chemiluminescence was developed according to the manufacturer's procedure (ECL; GE Healthcare).

Sandwich ELISA

The concentration of HE4 in culture media of cancer cell lines and donor sera was measured by a HE4-specific sandwich ELISA constructed as follows: 96-well microtiter plates (Nalge Nunc International Corp., Rochester, NY) were coated with the capturing antibody clone 110-108 with carbonate buffer at 4°C overnight. The plates were blocked with 200 μl PBS containing 1.0% BSA for 2 h and then incubated for 1 h with culture media diluted to 1:2 with sample diluent which consists of PBS containing 1.0% BSA and 0.1% Tween 20 or serum samples diluted to 1:10 with the same diluent and HRP-conjugated antibody 128-119 diluted to 1:140,000 with PBS containing BSA. After washing the plates with PBS containing Tween20, 100 μl/well TMB (Moss Inc., Pasadena, MD) was added, and the plates were incubated for 30 min at room temperature. The color development was stopped by the addition of H_2SO_4. Color intensity was determined at a wavelength of 450 nm with a reference wavelength of 620 nm. Analyte concentrations were calculated by referring to the standard curve using serial diluted recombinant HE4 (Fig. 1d).

Immunohistochemistry

Paraffin-embedded cancer tissue slices or noncancer tissue slices derived from lung cancer patients (adenocarcinoma and squamous cell carcinoma) were purchased from Outdo, Shanghai, China. The tissue slices were deparaffinized by treatment with xylene for 5 min three times, 100% ethanol for 5 min twice, 90% ethanol for 5 min once, 80% ethanol for 5 min once, 70% ethanol for 5 min once and PBS for 5 min three times. Subsequently, for an antigen retrieval, the specimens were immersed in a citrate buffer and heated by microwave for 10 min twice. In order to inactive the endogenous peroxidase activity, the specimens were then treated with PBS containing a 3% hydrogen peroxide solution at room temperature for 10 min. After washing with PBS twice, the specimens were blocked with blocking buffer and incubated with a blocking buffer containing 1 μg/ml of polyclonal HE4 antibody for 1 h at room temperature. After washing with PBS twice, the specimens were incubated with HRP-conjugated second antibody (EnVision Dual Link, Dako, Denmark) for 1 h at room temperature. Subsequently, the specimens were washed with PBS twice and allowed to react with a DAB chromogen (Dako) for 10 min at room temperature. The reaction was stopped by washing with water. After counterstaining with hematoxylene, the tissue slices were dehydrated with ethanol and xylene and made into specimens using a mounting medium (Matsunami Glass, Osaka, Japan).

Statistical analysis

To test for statistically significant differences between two groups, an unpaired Student's *t*-test was used. For comparisons among three or more groups, the values were analyzed by one-way ANOVA followed by Scheffe's post hoc comparisons. Differences were considered significant at $P<0.05$. For drawing of receiver operating characteristic (ROC) curves and estimation of the area under the ROC curve (AUC) statistics software SPBS (Comworks, Saitama, Japan) was used to quantify the ability to differentiate between

healthy volunteers and patients with lung cancer. Analyses of the prognostic impact of serum HE4 levels on survival from response evaluation to death or last follow-up used the Kaplan–Meier method and logrank test.

Results

Generation of ELISA specific for HE4

To generate monoclonal antibodies that specifically react with HE4, recombinant HE4 protein corresponding to the amino acids 1–124 of the transcript for human HE4 was produced by 293 T transfectants (Fig. 1a) and immunized to BALB/c mice. Supernatants of obtained hybridomas were tested for binding activity to microplates coated with immunizing antigen and further examined by a competition assay for the immunogen (data not shown). The specific reactivities of selected clone 13F5G1, 99-44, 110-108, 128-119, 179-137 and 201-50 to HE4 were checked by immunoprecipitation using myc-His-tagged recombinant HE4 (Fig. 1b). The specificity of 110-108 and 128-119 to HE4 was tested using the 293 T transfectant-expressing HE4 by flowcytometory. Clones 110-108 and 128-119 detected the antigen on the cell surface of 293 T transfectant (Fig. 1c). A sandwich ELISA for HE4 was constructed using the anti-HE4 antibodies 110-108 and 128-119. The standard curve using purified recombinant HE4 is shown in Fig. 1d. The HE4 sandwich ELISA detected the antigen in the culture supernatant of the various types of cancer cell lines (Fig. 1e). We investigated immunohistochemical staining of lung cancer tissue using anti-HE4 antibody. HE4 expression was detected in lung cancer tissues but not in normal lung tissues. We compared HE4 staining between adenocarcinoma and squamous cell carcinoma lung tissue samples but could not detect significant differences in staining intensity. Furthermore, we could not find a correlation between differentiation and HE4 staining of lung cancer tissues. Strong HE4 staining was

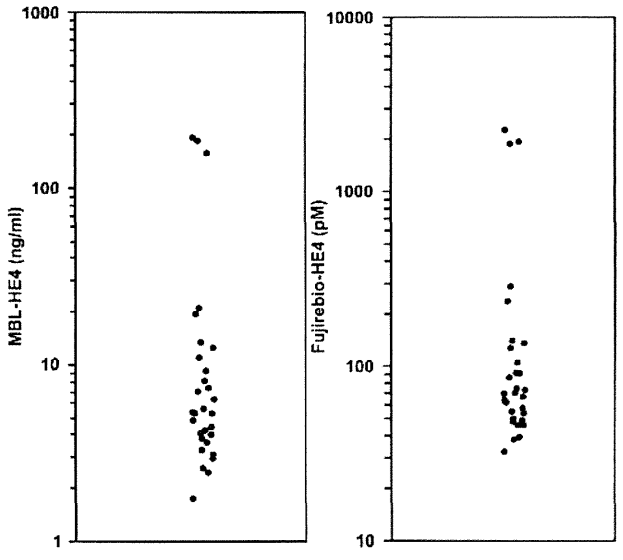

Fig. 2 HE4 levels in sera of ovarian cancer patients. HE4 levels determined by our ELISA system (*left*) and Fujirebio commercial ELISA kit (*right*). Each *dot* represents one patient

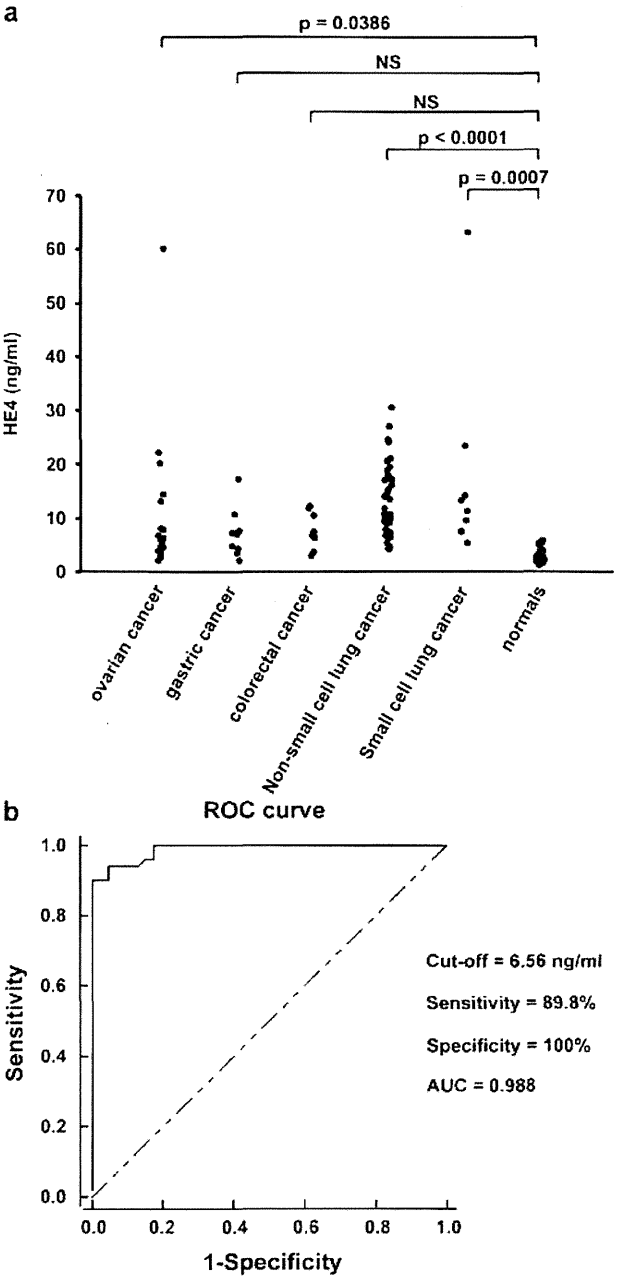

Fig. 3 a HE4 levels in the sera of cancer patients and normal controls. Each dot represents one patient. *NS* no significant. b Receiver operating characteristic (ROC) curves for HE4 for differentiation between lung cancer and healthy volunteers. The tables show the best statistical cutoff values for HE4 with pairs of sensitivity and specificity

Table 3 Pre- and post-treatment HE4 in lung cancer patients

Clinical response	Number of patients	Pre-treatment HE4 (ng/ml)			Post-treatment HE4 (ng/ml)		
		Mean (SD)	Median	Range	Mean (SD)	Median	Range
PR	8	23.0 (26.3)	14.2	8.3–86.5	12.6 (2.8)	12.9	8.2–16.1
SD	11	22.2 (32.3)	11.4	3.7–116.6	28.3 (44.4)	14.2	3.7–158.1
PD	5	21.3 (7.3)	22.8	9.3–28.1	23.8 (5.9)	25.9	14.2–29.1

detected in cytoplasmic and plasma membrane areas but not in nuclear area (Fig. 1f).

Evaluation of ELISA system

To assess the clinical potential of our ELISA system, we compared our ELISA system with an existing commercial ELISA kit (Fujirebio Diagnostics, Malvern, PA). We set the cutoff point of the existing ELISA kit as 150 pM based on the manufacturer's instructions (94.4 percentile of healthy individuals). In accordance with the existing ELISA kit, we set the cutoff point of our ELISA system as 5.5 ng/ml based on 94.4 percentile of 37 healthy individuals. We measured concentrations of HE4 of ovarian cancer patients by using two ELISA and found that our ELISA system shows better sensitivity for diagnosis of ovarian cancer than the existing ELISA kit by Fisher's exact probability test ($p<0.05$) (Fig. 2).

Diagnostic value of HE4

We measured serum HE4 levels in cancer patients and healthy controls by using our ELISA system. Mean serum HE4 levels in patients with non-small cell lung cancer, small cell lung cancer, ovarian cancer, gastric cancer, colorectal cancer and healthy adults were 13.3 ng/ml, 17.3 ng/ml, 10.9 ng/ml, 7.2 ng/ml, 7.7 ng/ml and 2.7 ng/ml (Table 1). Serum HE4 levels were significantly higher for non-small, small cell lung cancer and ovarian cancer patients than for healthy controls ($p<0.0001$, $p=0.0007$, and $p=0.0386$, respectively) (Fig. 3a).

To assess the clinical potential of HE4, we calculated sensitivities and specificities of HE4. The operating characteristics for HE4 with its cutoff points for achieving the best individual accuracy are shown in Fig. 3b. The AUC for serum HE4 was 0.988 for differentiating lung cancer patients from healthy adults, with a cutoff value of 6.56 ng/ml (sensitivity= 89.8%, specificity=100%) (Fig. 3b). Serum HE4 levels were elevated in 36/40 (90.0%) non-small cell lung cancer patients, 8/9 (88.9%) small cell lung cancer patients, 8/18 (44.4%) ovarian cancer patients, 6/10 (60.0%) gastric cancer patients and 5/8 (62.5%) colorectal cancer patients (Table 1). These results suggest that the sensitivity of HE4 was high in lung cancer patients.

Prognostic value of HE4

Pre- and post-treatment mean HE4 were 23.0 ng/ml (range 8.3–86.5 ng/ml) and 12.6 ng/ml (range 8.2–16.1 ng/ml), respectively, for PR patients, whereas 21.3 ng/ml (range 9.3–28.1 ng/ml) and 23.8 ng/ml (range 14.2–29.1 ng/ml), respectively, for PD patients (Table 3). Post-treatment mean

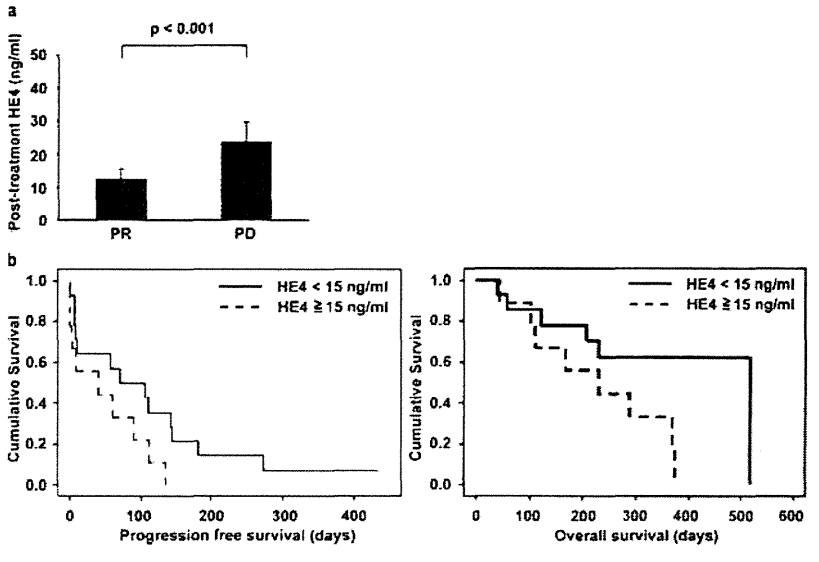

Fig. 4 **a** Post-treatment serum HE4 levels of lung cancer patients receiving chemotherapy. Figures show the average (*columns*) + SD (*bars*). **b** Kaplan–Meier plots of overall survival (*right*) and progression-free survival (*left*) after chemotherapy

HE4 in PR patients was significantly lower than that in PD patients ($p<0.001$) (Fig. 4a). Overall median survival after treatment was 9.6 months. Post-treatment HE4 levels were above the cutoff limit (15 ng/ml) in one of eight for PR and in four of five for PD patients. We divided patients into high (>15 ng/ml) and low (<15 ng/ml) HE4 groups post-treatment. We set the cutoff point at 15 ng/ml based on the median value of HE4 levels. Median overall survival of low HE4 group was significantly longer than that of high HE4 group (17.3 vs. 7.7 months; $p<0.05$) (Fig. 4b). Median progression-free survival after chemotherapy for low HE4 group was 2.4 months, compared with 1.4 months for high HE4 group ($p=0.083$) (Fig. 4b).

Discussion

In our study, we developed a novel ELISA system to detect serum HE4, and by using this system, we show that HE4 has potential as a diagnostic marker of lung cancer. Specifically, we found that serum HE4 levels in lung cancer patients after chemotherapy is strongly correlated with survival after the treatment.

Our HE4 ELISA shows better sensitivity for diagnosis of ovarian cancer than the existing HE4 ELISA kit. Furthermore, there are two advantages to our HE4 ELISA over the existing HE4 ELISA kit. First, while the existing ELISA kit is designed to use undiluted serum as the test sample, using our system, a small sample volume can be applied to our ELISA to detect HE4 in human serum. A diluted sample, maximally five times dilution, can be used in our assay system. This is of practical importance when simultaneous measures of other biomarkers are required from one serum sample. Second, a simpler and more rapid test is achieved using our HE4 ELISA. Test duration for our HE4 ELISA is approximately half of the time required by the existing HE4 ELISA kit. The existing HE4 ELISA kit requires a shaking procedure during reaction of antibody to the sample, while our new ELISA incubates the sample with antibody in a stationary condition. Thus, our HE4 ELISA does not require the purchase of specialized equipment for shaking incubation.

We evaluated the diagnostic efficacy of HE4 in lung, ovarian, gastric and colorectal cancer patients and found that HE4 indicated high sensitivity in lung cancer patients. Tissue expression of HE4 has been reported to be increased in pulmonary, ovarian and gastrointestinal carcinomas [15–18, 20, 21]. HE4 as a serum marker was mainly investigated in ovarian cancer patients and was shown to be a promising diagnostic marker [22]. We show that serum HE4 levels were significantly higher for not only ovarian cancer but also lung cancer patients than for healthy controls. Escudero et al. previously measured HE4 concentrations in patients with various types of malignant diseases and found that HE4 concentrations were abnormal primarily in gynecologic cancer and lung cancer [23]. Taken together, these data HE4 may be considered to be a potential diagnostic marker of lung cancer.

In this study, we found that post-treatment HE4 level is correlated with survival after chemotherapy. It was reported that high levels of serum HE4 is significantly correlated with worse prognosis in epithelial ovarian cancer patients [24]. Yamashita et al. reported that HE4 expression by immunohistochemistry staining is significantly correlated with prognosis in lung adenocarcinoma patients [25]. There is a growing need for diagnostic tools to estimate the prognosis of the patient, to monitor the treatment course and to early detect the response to therapy, which would help to optimize disease management on an individual basis. Our results suggest that serum HE4 is a promising prognostic marker. To our knowledge, this is the first time that the potential prognostic impact of serum HE4 in lung cancer patients has been investigated. We are aware of the small cohort of patients in this study, and thus, further study by larger scale prospective trials will be needed.

In conclusion, we used ELISA systems developed by us to detect significant differences in the levels of serum HE4 between lung cancer patients and normal controls. In addition, it is suggested that HE4 is correlated with prognosis after chemotherapy. We are planning a further study to evaluate serum HE4 for a diagnostic and prognostic marker by larger scale of patients.

Acknowledgments We appreciate Shintaro Nomura (Nagahama Institute of Bio-Science and Technology, Shiga, Japan) for providing helpful comments on immunohistochemical analysis, Barry Ripley for outstanding editing of the manuscript and Masako Ikeda for their technical assistance. We wish to thank Y. Ito, N. Kawakami and Y. Kanazawa for their secretarial assistance. This work was supported by a grant-in-aid from the Ministry of Health, Labour and Welfare, Japan.

Conflict of interest None.

References

1. Jemal A, Siegel R, Xu J, Ward E. Cancer statistics, 2010. CA Cancer J Clin. 2010;60:277–300.
2. Fruh M. The search for improved systemic therapy of non-small cell lung cancer—what are today's options? Lung Cancer. 2011;72:265–70.
3. Martini N, Kris MG, Gralla RJ, Bains MS, McCormack PM, Kaiser LR, Burt ME, Zaman MB. The effects of preoperative chemotherapy on the resectability of non-small cell lung carcinoma with mediastinal lymph node metastases (n2 m0). Ann Thorac Surg. 1988;45:370–9.
4. Shinkai T, Saijo N, Tominaga K, Eguchi K, Shimizu E, Sasaki Y, Fujita J, Futami H, Ohkura H, Suemasu K. Serial plasma carcinoembryonic antigen measurement for monitoring patients with advanced lung cancer during chemotherapy. Cancer. 1986;57:1318–23.

5. Pujol JL, Grenier J, Daures JP, Daver A, Pujol H, Michel FB. Serum fragment of cytokeratin subunit 19 measured by cyfra 21-1 immunoradiometric assay as a marker of lung cancer. Cancer Res. 1993;53:61–6.
6. Miyake Y, Kodama T, Yamaguchi K. Pro-gastrin-releasing peptide (31-98) is a specific tumor marker in patients with small cell lung carcinoma. Cancer Res. 1994;54:2136–40.
7. Kirchhoff C, Habben I, Ivell R, Krull N. A major human epididymis-specific cDNA encodes a protein with sequence homology to extracellular proteinase inhibitors. Biol Reprod. 1991;45:350–7.
8. Kirchhoff C. Molecular characterization of epididymal proteins. Rev Reprod. 1998;3:86–95.
9. Wang K, Gan L, Jeffery E, Gayle M, Gown AM, Skelly M, Nelson PS, Ng WV, Schummer M, Hood L, Mulligan J. Monitoring gene expression profile changes in ovarian carcinomas using cDNA microarray. Gene. 1999;229:101–8.
10. Schummer M, Ng WV, Bumgarner RE, Nelson PS, Schummer B, Bednarski DW, Hassell L, Baldwin RL, Karlan BY, Hood L. Comparative hybridization of an array of 21,500 ovarian cDNAs for the discovery of genes overexpressed in ovarian carcinomas. Gene. 1999;238:375–85.
11. Hough CD, Sherman-Baust CA, Pizer ES, Montz FJ, Im DD, Rosenshein NB, Cho KR, Riggins GJ, Morin PJ. Large-scale serial analysis of gene expression reveals genes differentially expressed in ovarian cancer. Cancer Res. 2000;60:6281–7.
12. Ono K, Tanaka T, Tsunoda T, Kitahara O, Kihara C, Okamoto A, Ochiai K, Takagi T, Nakamura Y. Identification by cDNA microarray of genes involved in ovarian carcinogenesis. Cancer Res. 2000;60:5007–11.
13. Welsh JB, Zarrinkar PP, Sapinoso LM, Kern SG, Behling CA, Monk BJ, Lockhart DJ, Burger RA, Hampton GM. Analysis of gene expression profiles in normal and neoplastic ovarian tissue samples identifies candidate molecular markers of epithelial ovarian cancer. Proc Natl Acad Sci U S A. 2001;98:1176–81.
14. Shridhar V, Lee J, Pandita A, Iturria S, Avula R, Staub J, Morrissey M, Calhoun E, Sen A, Kalli K, Keeney G, Roche P, Cliby W, Lu K, Schmandt R, Mills GB, Bast Jr RC, James CD, Couch FJ, Hartmann LC, Lillie J, Smith DI. Genetic analysis of early- versus late-stage ovarian tumors. Cancer Res. 2001;61:5895–904.
15. Schaner ME, Ross DT, Ciaravino G, Sorlie T, Troyanskaya O, Diehn M, Wang YC, Duran GE, Sikic TL, Caldeira S, Skomedal H, Tu IP, Hernandez-Boussard T, Johnson SW, O'Dwyer PJ, Fero MJ, Kristensen GB, Borresen-Dale AL, Hastie T, Tibshirani R, van de Rijn M, Teng NN, Longacre TA, Botstein D, Brown PO, Sikic BI. Gene expression patterns in ovarian carcinomas. Mol Biol Cell. 2003;14:4376–86.
16. Lu KH, Patterson AP, Wang L, Marquez RT, Atkinson EN, Baggerly KA, Ramoth LR, Rosen DG, Liu J, Hellstrom I, Smith D, Hartmann L, Fishman D, Berchuck A, Schmandt R, Whitaker R, Gershenson DM, Mills GB, Bast Jr RC. Selection of potential markers for epithelial ovarian cancer with gene expression arrays and recursive descent partition analysis. Clin Cancer Res. 2004;10:3291–300.
17. Drapkin R, von Horsten HH, Lin Y, Mok SC, Crum CP, Welch WR, Hecht JL. Human epididymis protein 4 (he4) is a secreted glycoprotein that is overexpressed by serous and endometrioid ovarian carcinomas. Cancer Res. 2005;65:2162–9.
18. Rosen DG, Wang L, Atkinson JN, Yu Y, Lu KH, Diamandis EP, Hellstrom I, Mok SC, Liu J, Bast Jr RC. Potential markers that complement expression of ca125 in epithelial ovarian cancer. Gynecol Oncol. 2005;99:267–77.
19. Hellstrom I, Raycraft J, Hayden-Ledbetter M, Ledbetter JA, Schummer M, McIntosh M, Drescher C, Urban N, Hellstrom KE. The he4 (wfdc2) protein is a biomarker for ovarian carcinoma. Cancer Res. 2003;63:3695–700.
20. Bingle L, Cross SS, High AS, Wallace WA, Rassl D, Yuan G, Hellstrom I, Campos MA, Bingle CD. Wfdc2 (he4): a potential role in the innate immunity of the oral cavity and respiratory tract and the development of adenocarcinomas of the lung. Respir Res. 2006;7:61.
21. Galgano MT, Hampton GM, Frierson Jr HF. Comprehensive analysis of he4 expression in normal and malignant human tissues. Mod Pathol. 2006;19:847–53.
22. Li J, Dowdy S, Tipton T, Podratz K, Lu WG, Xie X, Jiang SW. He4 as a biomarker for ovarian and endometrial cancer management. Expert Rev Mol Diagn. 2009;9:555–66.
23. Escudero JM, Auge JM, Filella X, Torne A, Pahisa J, Molina R. Comparison of serum human epididymis protein 4 with cancer antigen 125 as a tumor marker in patients with malignant and nonmalignant diseases. Clin Chem. 2011;57:1534–44.
24. Steffensen KD, Waldstrom M, Brandslund I, Jakobsen A. Prognostic impact of prechemotherapy serum levels of her2, ca125, and he4 in ovarian cancer patients. Int J Gynecol Canc. 2011;21:1040–7.
25. Yamashita S, Tokuishi K, Hashimoto T, Moroga T, Kamei M, Ono K, Miyawaki M, Takeno S, Chujo M, Yamamoto S, Kawahara K. Prognostic significance of he4 expression in pulmonary adenocarcinoma. Tumour Biol. 2011;32:265–71.

TOPICS

Serum leucine-rich alpha-2 glycoprotein is a disease activity biomarker in ulcerative colitis

Serada S, Fujimoto M, Terabe F, Iijima H, Shinzaki S, Matsuzaki S, Ohkawara T, Nezu R, Nakajima S, Kobayashi T, Plevy SE, Takehara T, Naka T

〔Inflamm Bowel Dis 2012；18：2169-2179 掲載〕

潰瘍性大腸炎の疾患活動性マーカーとしての血清ロイシンリッチアルファ2グリコプロテイン

世良田 聡* 藤本 穣* 仲 哲治*
Satoshi Serada Minoru Fujimoto Tetsuji Naka

Key words：炎症性腸疾患，潰瘍性大腸炎，バイオマーカー

論文の背景

炎症性腸疾患(inflammatory bowel disease：IBD)は再燃と寛解を繰り返す原因不明の慢性炎症性疾患であり，潰瘍性大腸炎(ulcerative colitis：UC)とクローン病(Crohn's disease：CD)に分類される．近年，IBDに対する免疫抑制薬，調節薬などを用いた治療法に加え，IBDの病態と関係の深いサイトカインの一つであるTNF-αを標的とした抗体医薬など生物学的製剤が使用され始めたことによって劇的な治療効果が発揮されたことにより，寛解を目指した治療が現実になりつつある[1),2)]．IBDの診療においては，内視鏡検査・X線検査などの画像診断，生検組織の病理学的診断といった炎症局所の評価が重要であることは明白であるが，これらの評価法以外にも，バイオマーカーの測定を併用することで炎症性腸疾患の診断や治療が低侵襲的，簡便で客観的，かつ低コストで行える可能性がある．

CDの疾患活動性を把握する活動性マーカーとしてはC-reactive protein(CRP)，赤沈検査(ESR)，白血球数などが知られている．これらの検査マーカーはCDの炎症局所である腸以外の炎症においても高値を示す．また，UCにおいてはこれらのマーカーはCDほど有用ではないといわれている[3)]．さらに，UCの疾患活動性を評価するために内視鏡的な所見は重要な情報であるが，内視鏡による検査は侵襲性が高いことが問題であり，短期間に繰り返して検査することが困難である．そのため，UCの治療に伴う疾患活動性の適切な評価を行うに当たり，侵襲性が少ない新規疾患活動性マーカーが必要とされている．

筆者らはこれまでにインフリキシマブ(TNF-α阻害抗体)治療前と治療後の関節リウマチ同一患者血清に対して定量的プロテオミクス手法を用

*独立行政法人医薬基盤研究所創薬基盤研究部免疫シグナルプロジェクト(〒567-0085 大阪府茨木市彩都あさぎ7-6-8)
* Laboratory for Immune Signal, National Institute of Biomedical Innovation, 7-6-8 Saito-Asagi, Ibaraki-city, Osaka 567-0085, Japan

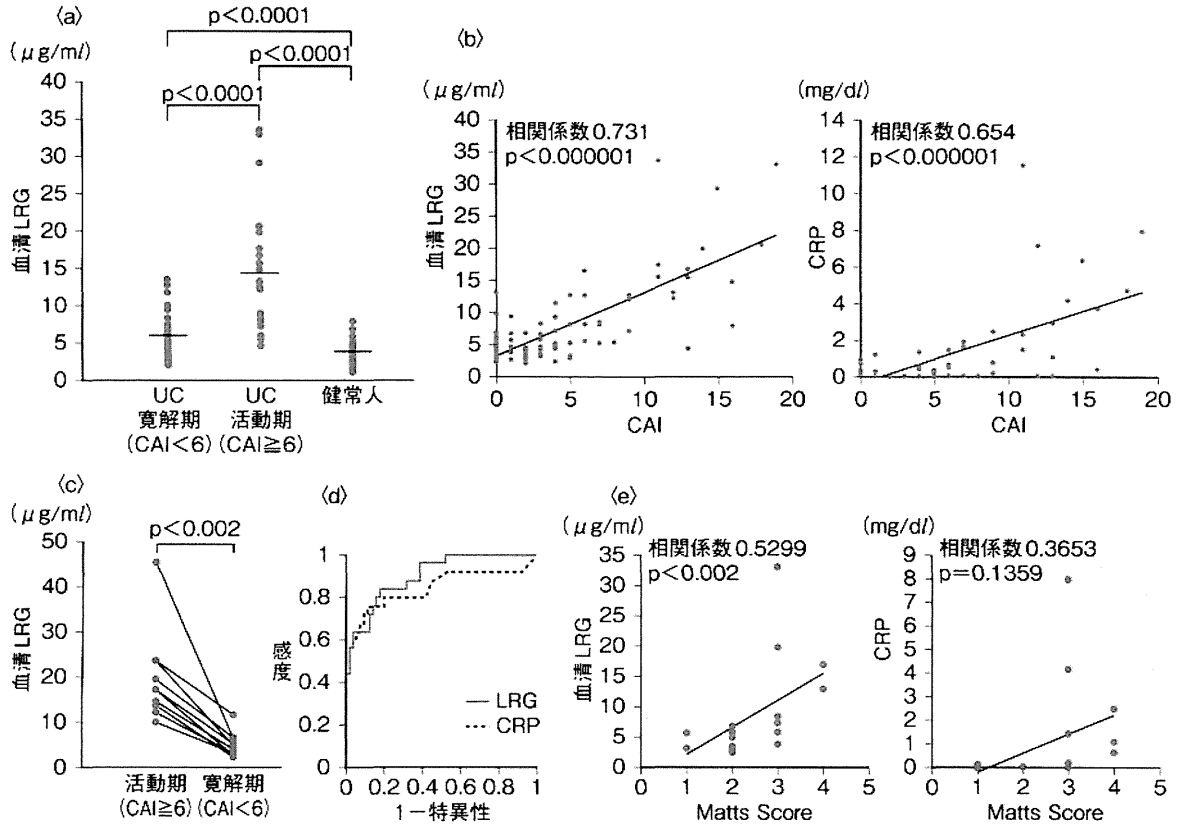

図　潰瘍性大腸炎の疾患活動性マーカーとしての leucine-rich α-2 glycoprotein (LRG) の有用性

a：潰瘍性大腸炎患者血清中の LRG 濃度
b：血清 LRG 濃度，および CRP と CAI との相関
c：活動期，寛解期における血清 LRG 濃度の変動
d：活動期と寛解期を区別する血清 LRG 濃度と CRP の ROC 曲線解析
e：血清 LRG 濃度，および CRP と内視鏡スコア (Matts Score) との相関
CAI：clinical activity index, ROC：receiver operating characteristic
〔Serada S, et al：Inflamm Bowel Dis 2012；18：2169-2179 より改変〕

いることで，治療によって発現変動を示す血清タンパク質を網羅的に探索した．その結果，CRP や serum amyloid A (SAA) のような既知の炎症マーカータンパク質のみならず，leucine-rich alpha-2 glycoprotein (LRG) というタンパク質が治療後よりも治療前にて高値を示すことを明らかにした[1]．LRG は 1977 年に発見された血清中に存在する糖タンパク質で，ロイシンリッチリピートと呼ばれる特徴的なドメインを八つ含むタンパク質であるが，生理的機能はまだ明らかにされていない[5]．疾患活動性マーカーとしての血清 LRG の有用性を検討するため，ELISA 法を用いて関節リウマチ患者血清中の LRG を定量した結果，LRG は関節リウマチの優れた疾患活動性マーカーとなりうることを明らかにした．さらに，血清 LRG が CD においても優れた疾患活動性マーカーとなりうることを明らかにしている．本論文は UC の疾患活動性マーカーとしての血清 LRG

の有用性について報告している.

論文の概要

UC患者82例を対象とし，血清中のLRG濃度をELISA法により定量した．その結果，血清LRG濃度は活動期(25例)において，寛解期(57例)，および健常人(50例)の血清LRG濃度よりも有意に高値を示した(図a)．UCの疾患活動性スコアであるClinical Activity Index(CAI)と血清LRG濃度との相関を解析した．その結果，血清LRG濃度はCRPよりもCAIと強く有意に相関した(図b)．さらに，寛解期の患者血清中のLRG濃度は活動期に比較して有意な低下を認めた(図c)．また，receiver operating characteristic (ROC)曲線解析から，UC活動期と寛解期を区別するマーカーとして血清LRG濃度はCRPよりも優れていた(図d)．UCの炎症の状態を把握するうえで内視鏡所見は直接的な指標となる．そこで，血清LRG濃度と内視鏡スコア(Matts Score)との相関を解析した．その結果，血清LRG濃度はCAIだけでなく内視鏡スコアに対してもCRPよりも強く相関関係を示した(図e)．また，LRGは炎症局所の腸組織において高発現することが免疫組織化学染色法にて確認された．LRGは正常腸組織からは発現がほとんどみられないものの，UC患者の炎症局所である腸組織において高発現するため，疾患活動性とより強く相関することが示唆されており，この点は炎症時に肝臓から産生されるCRPと異なった特徴と考えられる．

IL-6欠損マウスを用いて炎症性腸疾患モデルの血清LRG濃度を解析した．その結果，野生型マウス，IL-6欠損マウスのいずれにおいてもdextran sulfate sodium(DSS)誘導性腸炎を誘導することにより血清LRG濃度の上昇が野生型マウスとIL-6欠損マウスの間において同程度で認められた．このことから，LRGの発現にはIL-6が必ずしも必要ではないことが明らかとなり，従来の炎症マーカーとして使用されているCRPとは発現調節機序が異なることが判明した．

以上の結果，血清LRGはCRPとは異なるUCの新規疾患活動性マーカーとなりうることが明らかとなった．興味深いことに，血清LRGはIL-6非依存性の発現調節機序が存在する炎症マーカーとなりうる．このことより，IL-6阻害療法を受けるためCRP値が常に陰性化するため，CRPを疾患活動性マーカーや感染症検出マーカーとして使えない関節リウマチなどの自己免疫疾患患者において，LRGが疾患活動性マーカー，あるいは感染症を検出できる有用性の高いマーカーとなることが期待される．

文　献

1) Feagan BG, Reinisch W, Rutgeerts P, et al : The effects of infliximab therapy on health-related quality of life in ulcerative colitis patients. Am J Gastroenterol 2007 ; 102 : 794-802
2) Fiorino G, Peyrin-Biroulet L, Repici A, et al : Adalimumab in ulcerative colitis : hypes and hopes. Expert Opin Biol Ther 2011 ; 11 (1) : 109-116
3) Vermeire S, Van Assche G, Rutgeerts P : Laboratory markers in IBD : useful, magic, or unnecessary toys? Gut 2006 ; 55 : 426-431
4) Serada S, Fujimoto M, Ogata A, et al : iTRAQ-based proteomic identification of leucine-rich alpha-2 glycoprotein as a novel inflammatory biomarker in autoimmune diseases. Ann Rheum Dis 2010 ; 69 : 770-774
5) Haupt H, Baudner S : Isolation and characterization of an unknown, leucine-rich 3.1-S-alpha2-glycoprotein from human serum. Hoppe Seylers Z Physiol Chem 1977 ; 358 : 639-646

Key words : inflammatory bowel diseases, ulcerative colitis, biomarker

Laboratory of Biopharmaceutical Research[1], National Institute of Biomedical Innovation; Laboratory of Toxicology and Safety Science[2], Graduate School of Pharmaceutical Sciences; The Center for Advanced Medical Engineering and Informatics[3]; Laboratory of Biomedical Innovation[4], Graduate School of Pharmaceutical Sciences, Osaka University, Osaka, Japan

Rho GDP-dissociation inhibitor alpha is associated with cancer metastasis in colon and prostate cancer

T. YAMASHITA[1,2,*], T. OKAMURA[1,*], K. NAGANO[1,*], S. IMAI[1], Y. ABE[1], H. NABESHI[1,2], T. YOSHIKAWA[1,2], Y. YOSHIOKA[1,2,3], H. KAMADA[1,3], Y. TSUTSUMI[1,2,3], S. TSUNODA[1,3,4]

Received July 7, 2011, accepted August 5, 2011

Shin-ichi Tsunoda, Ph.D, Laboratory of Biopharmaceutical Research, National Institute of Biomedical Innovation, 7-6-8 Saito-Asagi, Ibaraki, Osaka 567-0085, Japan.
tsunoda@nibio.go.jp
**These authors contributed equally to the work.*

Pharmazie 67: 253–255 (2012) *doi: 10.1691/ph.2012.1630*

Since metastasis is one of the most important prognostic factors in colorectal cancer, development of new methods to diagnose and prevent metastasis is highly desirable. However, the molecular mechanisms leading to the metastatic phenotype have not been well elucidated. In this study, a proteomics-based search was carried out for metastasis-related proteins in colorectal cancer by analyzing the differential expression of proteins in primary versus metastasis focus-derived colorectal tumor cells. Protein expression profiles were determined using a tissue microarray (TMA), and the results identified Rho GDP-dissociation inhibitor alpha (Rho GDI) as a metastasis-related protein in colon and prostate cancer patients. Consequently, Rho GDI may be useful as a diagnostic biomarker and/or a therapeutic to prevent colon and prostate cancer metastasis.

1. Introduction

Colorectal cancer is known as a major metastatic cancer, and 40–50% of patients already have a metastatic focus at presentation. Moreover, the 5-year survival of these patients is under 10% (Davies et al. 2005). Thus, metastasis is one of the most important prognostic factors in colorectal cancer. In order to improve rates of cancer remission, it will be necessary to clarify the detailed molecular mechanisms of cancer metastasis and to utilize this information to establish new diagnostic and therapeutic techniques. Many researchers have searched for metastasis-related molecules (Liu et al. 2010; Shuehara et al. 2011) using proteomics techniques (Hanash 2003). Comprehensive mapping of the molecular changes during metastasis would greatly improve our understanding of the recurrence and management of cancer. However, the knowledge gained so far in these studies has not been sufficient to improve cancer remission rates.

Here we show the potential of Rho GDI as a metastasis-related protein in colon and prostate cancer patients. In order to identify metastasis-related proteins, the protein expression patterns of human colorectal cancer cells with different metastatic characters were compared. Because these cells were derived from the same patient (SW480: a surgical specimen of a primary colon adenocarcinoma, SW620: a lymph node metastatic focus), cancer metastasis-related protein candidates could be effectively sought without background variations due to differences between individuals. Furthermore, by analyzing the expression of candidate proteins in many clinical samples using a TMA, we attempted to validate the association of these candidates with metastasis. TMA is a slide glass containing many clinical tissues, and it enables one to carry out a high-throughput analysis by evaluating the relationship between expression profiles of each candidate molecule and clinical information such as metastasis. (Imai et al. 2011; Yoshida et al. 2011).

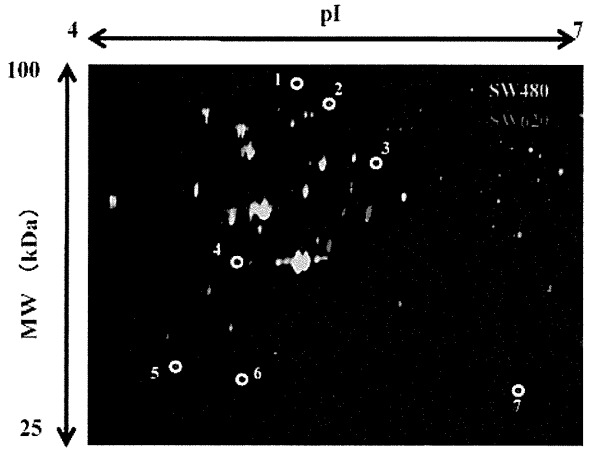

Fig. 1: 2D-DIGE image of fluorescently-labeled proteins from different metastatic human colorectal cancer cells. SW480 is human colorectal cancer cell line derived from a primary tumor and SW620 is derived from a metastatic focus from the same patient. Proteins from the colon cancer cells (SW480, SW620) were labeled with Cy3 and Cy5 respectively, and analyzed by 2D electrophoresis. The differentially-expressed spots (white circles) were then identified by LC-UHR TOF/MS

Table 1: High expression proteins in SW620 compared to SW480

	Accession	Protein name	MW (kDa)	pI	Ratio (SW620 / SW480)
1	P12109	collagen alpha-1(VI) chain	108.6	5.3	1.53
2	Q15459	splicing factor 3A subunit 1	88.9	5.2	1.61
3	P13797	T-plastin	70.9	5.5	1.59
4	P60709	actin cytoplasmic 1	42.1	5.3	1.50
5	P63104	14-3-3 zeta/delta	27.9	4.7	1.63
6	P52565	Rho GDP-dissociation inhibitor 1 (Rho GDI)	23.3	5.0	1.90
7	P30041	Peroxiredoxin-6 (PRDX6)	25.1	6.0	1.86

2. Investigations, results and discussion

In order to search for metastasis-related proteins, we analyzed differentially-expressed proteins between SW480 and SW620 by two-dimensional differential in-gel electrophoresis (2D-DIGE) (Fig. 1). As a result, 7 spots with at least a 1.5-fold-altered expression level were found by quantitative analysis, and these spots were identified by mass spectrometry (Table 1). Three molecules having a high SW620/SW480 expression ratio indicating a strong association with cancer metastasis were identified: Rho GDP-dissociation inhibitor alpha (Rho GDI), peroxiredoxin-6 (PRDX6) and 14-3-3 zeta/delta.

The expression profiles of these proteins were analyzed by immunohistochemistry using the TMA with colon cancer and multiple cancer tissues. Results of this analysis indicated that expression of PRDX6 and 14–3-3 zeta/delta had no relationship to the clinical status of cancer metastasis (data not shown). On the other hand, in positive cases of lymph node metastasis, the expression ratio of Rho GDI was significantly higher than in the negative cases. Furthermore, the same trend was seen when tissues from prostate cancer patients were analyzed (Table 2).

To confirm these results, the expression levels of Rho GDI protein in colon cancer cell lines with different metastatic potential (SW480 < SW620 < SW620-OK1 < SW620-OK2: Characteristics of SW620-OK1 and SW620-OK2 are described in *Experimental*) were investigated by western blot analysis (Fig. 2). The expression of Rho GDI was found to be up-regulated with the development of metastatic characteristics. These results suggested that Rho GDI is correlated with cancer metastasis.

Rho GDI has been identified as key regulator of Rho family GTPases. Activation of growth factor receptors and integrins can promote the exchange of GDP for GTP on Rho proteins (Bishop et al. 2000). Furthermore, GTP-bound Rho proteins interact with a range of effector molecules to modulate their activity or localization, and this leads to changes in cell behavior. It is clear that Rho family GTPases are involved in the control of cell morphology and motility (Etienne-Manneville et al. 2002; Hall et al. 1997; Van Aelst et al. 1997). The importance of Rho protein and Rho GDI in cancer progression, particularly in the area of metastasis, is becoming increasingly evident. Recently, some reports have indicated that the expression of Rho GDI was correlated with colorectal and breast cancer metastasis (Zhao et al. 2008; Kang et al. 2010). Thus, our findings are consistent with these reports and further suggest that the expression of Rho GDI is also correlated with prostate cancer metastasis. Consequently, Rho GDI should be considered as a diagnostic marker or new therapeutic target for cancer metastasis.

3. Experimental

3.1. Cell lines

SW480 is a human colorectal cancer cell line derived from a primary focus and SW620 is derived from a metastatic focus of the same patient. These cells were purchased from American Type Culture Collection and maintained at 37 °C using Leibovitz's L-15 medium (Wako) supplemented with 10% FCS. SW620-OK1 and -OK2 were established by the following procedure: 1×10^6 SW620 cells were injected into the spleens of nu/nu mice. After 8 weeks, SW620-OK1 was established from a liver metastatic focus. Furthermore, SW620-OK2 was established from SW620-OK1 using the same procedures.

3.2. 2D-DIGE analysis

Cell lysates were prepared from SW480 and SW620 and then solubilized with 7 M urea, 2 M thiourea, 4% CHAPS and 10 mM Tris-HCl (pH 8.5). The lysates were labeled at the ratio of 50 μg proteins: 400 pmol Cy3 or Cy5 protein-labeling dye (GE Healthcare Biosciences) in dimethylformamide according to the manufacturer's protocol. Briefly, the labelled samples were mixed with rehydration buffer (7 M urea, 2 M thiourea, 4% CHAPS, 2% DTT, 2% Pharmalyte (GE Healthcare Biosciences)) and applied to a 24-cm immobilized pH gradient gel strip (IPG-strip pH 4–7 NL) for separation in the first dimension. Samples for the spot-picking gel were prepared without labelling by Cy-dyes. For the second dimension separation, the IPG-strips were applied to SDS-PAGE gels (10% polyacrylamide and 2.7% N,N'-diallyltartardiamide gels). After electrophoresis, the gels were scanned with a laser fluoroimager (Typhoon Trio, GE Healthcare Biosciences). The spot-picking gel was scanned after staining with Deep Purple Total Protein Stain (GE Healthcare Biosciences). Quantitative analysis of protein spots was carried out with Decyder-DIA software (GE Healthcare Biosciences). For the antigen spots of interest, spots of 1 mm × 1 mm in size were picked using Ettan Spot Picker (GE Healthcare Biosciences).

3.3. In-gel tryptic digestion

Picked gel pieces were digested with trypsin as described below. The gel pieces were destained with 50% acetonitrile/50 mM NH_4HCO_3 for 20 min twice, dehydrated with 75% acetonitrile for 20 min, and then dried using a centrifugal concentrator. Next, 5 μl of 20 μl/ml trypsin (Promega) solution was added to each gel piece and incubated for 16 h at 37 °C. Three solutions were used to extract the resulting peptide mixtures from the gel pieces. First, 50 μl of 50% (v/v) acetonitrile in 0.1% (v/v) formic acid (FA) was added to the gel pieces, which were then sonicated for 5 min. Next, we collected the solution and added 80% (v/v) acetonitrile in 0.1% FA. Finally, 100% acetonitrile was added for the last extraction. The peptides were dried and then re-suspended in 10 μl of 0.1% FA.

3.4. Mass spectrometry and database search

Extracted peptides were analyzed by liquid chromatography Ultra High Resolution time-of-flight mass spectrometry (LC-UHR TOF/MS; maXis, Bruker Daltonics). The Mascot search engine (http://www.matrixscience.com) was initially used to query the entire theoretical tryptic peptide database as well as SwissProt (http://www.expasy.org/, a public domain database pro-

Table 2: Expression profile of Rho GDI in primary cancers with or without lymph node metastasis

	Number of Rho GDI positive cases (positive ratio)	
	in metastasis negative cases	in metastasis positive cases
Colon cancer*	11/14 (79%)	19/19 (100%)
Prostate cancer*	18/23 (78%)	11/11 (100%)

* $p < 0.05$: Mann Whitney U test

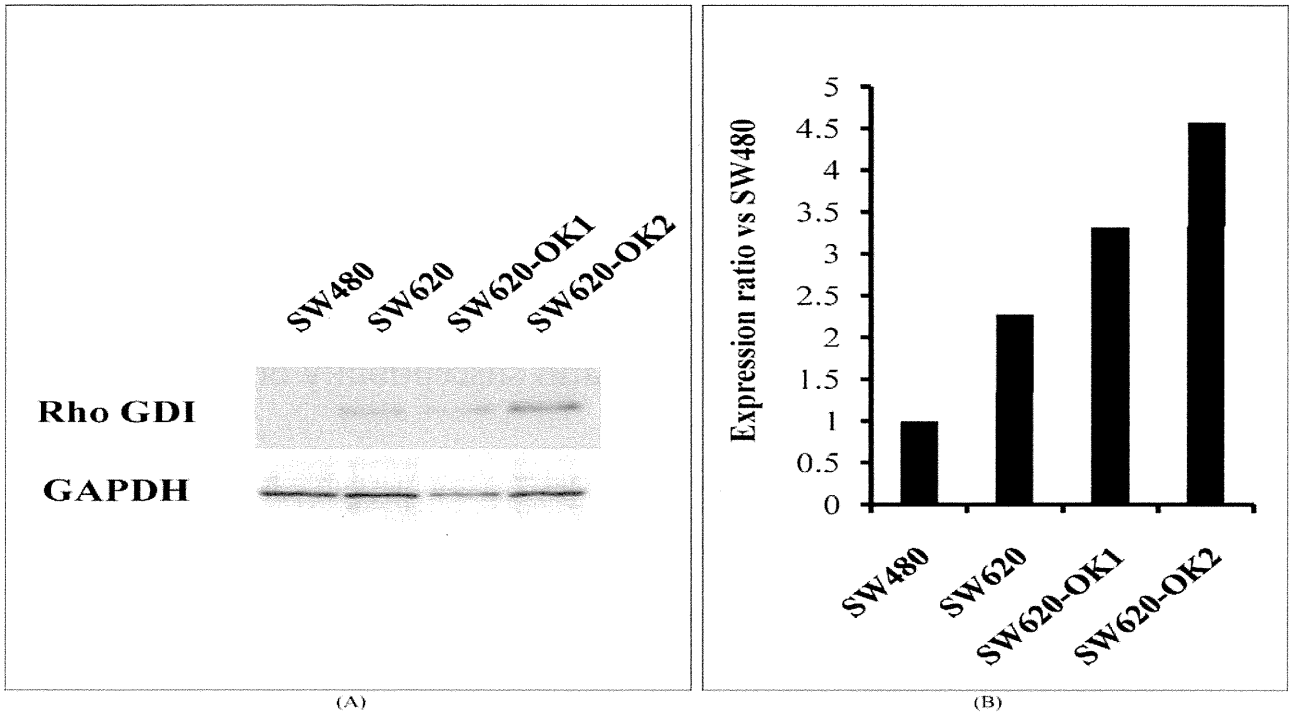

Fig. 2: Rho GDI expression levels in colon cancer cell lines with different metastatic abilities. Rho GDI expression levels in colon cancer cell lines (SW480, SW620, SW620-OK1, SW620-OK2) analyzed by western blotting (A). SW620-OK1, SW620-OK2 have been established as high metastatic sub-lines of SW620 using a mouse metastasis model. Intensity of the western blotting images was quantified by densitometry (B)

vided by the Swiss Institute of Bioinformatics). The search query assumed the following: (i) the peptides were monoisotopic (ii) methionine residues may be oxidized (iii) all cysteines are modified with iodoacetamide.

3.5. TMA Immunochemical staining

TMA slides with human colon cancer samples or multiple cancer samples (Biomax) were de-paraffinated in xylene and rehydrated in a graded series of ethanol washes. Heat-induced epitope retrieval was performed while maintaining the Target Retrieval Solution pH 9 (Dako) at the desired temperature according to manufacturer's instructions. After the treatment, endogenous peroxidase was blocked with 0.3% H_2O_2 in Tris-buffer saline (TBS) for 5 min. After washing twice with TBS, TMA slides were incubated with 10% BSA blocking solution for 30 min. The slides were then incubated with the anti-Rho GDI (Santa Cruz Biotechnology) for 60 min. After washing three times with wash buffer (Dako), each series of sections was incubated for 30 min with Envision + Dual Link (Dako). The reaction products were rinsed twice with wash buffer and then developed in liquid 3, 3'-diaminobenzidine (Dako) for 3 min. After the development, sections were counterstained with Mayer's hematoxylin. All procedures were performed using AutoStainer (Dako).

3.6. TMA Immunohistochemistry scoring

The optimized staining conditions for TMAs corresponding to human colon as well as multiple cancers were determined based on the co-existence of both positive and negative cells in the same tissue sample. Signals were considered positive when reaction products were localized in the expected cellular component. The criteria for scoring of stained tissues were as follows: the distribution score was 0 (0%), 1 (1–50%) or 2 (51–100%), indicating the percentage of positive cells among all tumor cells present in one tissue. The intensity of the signal (intensity score) was scored as 0 (no signal), 1 (weak), 2 (moderate) or 3 (marked). The distribution and intensity scores were then summed into a total score (TS) of TS0 (sum = 0), TS1 (sum = 2), TS2 (sum = 3), and TS3 (sum = 4–5). Throughout this study, TS0 or TS1 was regarded as negative, whereas TS2 or TS3 were regarded as positive.

3.7. Western Blot

Expression of Rho GDI in colon cancer cells was detected by anti-Rho GDI (Santa Cruz Biotechnology) and HRP conjugated anti-mouse IgG antibody (Sigma) using the ECL-plus system. Equal amounts of protein loading were confirmed by parallel β-actin immunoblotting, and signal quantification was performed by densitometric scanning.

Acknowledgements: This study was supported in part by Grants-in-Aid for Scientific Research from the Ministry of Education, Culture, Sports, Science and Technology of Japan, and from the Japan Society for the Promotion of Science (JSPS). This study was also supported in part by Health Labor Sciences Research Grants from the Ministry of Health, Labor and Welfare of Japan.

References

Bishop AL, Hall A (2000) Rho GTPases and their effector proteins. Biochem J 348: 241–255.

Davies RJ, Miller R, Coleman N (2005) Colorectal cancer screening: prospects for molecular stool analysis. Nat Rev Cancer 5: 199–209.

Etienne-Manneville S, Hall A (2002) Rho GTPases in cell biology. Nature 420: 629–635.

Hall A (1997). Rho GTPases and the Actin cytoskeleton. Science 279: 509–514.

Hanash S (2003) Disease proteomics. Nature 422: 226–232.

Imai S, Nagano K, Yoshida Y, Okamura T, Yamashita T, Abe Y, Yoshikawa T, Yoshioka Y, Kamada H, Mukai Y, Nakagawa S, Tsutsumi Y, Tsunoda S (2011). Development of an antibody proteomics system using a phage antibody library for efficient screening of biomarker proteins. Biomaterials 32: 162–169.

Kang S, Kim MJ, An H, Kim BG, Choi YP, Kang KS, Gao MQ, Park H, Na HJ, Kim HK, Yun HR, Kim DS, Cho NH (2010) Proteomic molecular portrait of interface zone in breast cancer. J Proteome Res 9: 5638–5645.

Liu R, Wang K, Yuan K, Wei Y, Huang C (2010) Integrative oncoproteomics strategies for anticancer drug discovery. Expert Rev Proteomics 7: 411–429.

Sahai E (2007). Illuminating the metastatic process. Nat Rev Cancer 7: 737–749.

Suehara Y, Tochigi N, Kubota D, Kikuta K, Nakayama R, Seki K, Yoshida A, Ichikawa H, Hasegawa T, Kaneko K, Chuman H, Beppu Y, Kawai A, Kondo T (2011) Secernin-1 as a novel prognostic biomarker candidate of synovial sarcoma revealed by proteomics. J Proteomics 74: 829–842.

Van Aelst L, D'Souza-Schorey C (1997) Rho GTPases and signaling networks. Genes Dev 11: 2295–2322.

Yoshida Y, Yamashita T, Nagano K, Imai S, Nabeshi H, Yoshikawa T, Yoshioka Y, Abe Y, Kamada H, Tsutsumi Y, Tsunoda S (2011) Limited expression of reticulocalbin-1 in lymphatic endothelial cells in lung tumor but not in normal lung. Biochem Biophys Res Commun 405: 610–614.

Zhao L, Wang H, Li J, Liu Y, Ding Y (2008) Overexpression of Rho GDP-dissociation inhibitor alpha is associated with tumor progression and poor prognosis of colorectal cancer. J Proteome Res 7: 3994–4003.

Biochemical and Biophysical Research Communications 421 (2012) 140–144

Contents lists available at SciVerse ScienceDirect

Biochemical and Biophysical Research Communications

journal homepage: www.elsevier.com/locate/ybbrc

Annexin A4 is a possible biomarker for cisplatin susceptibility of malignant mesothelioma cells

Takuya Yamashita [a,b,1], Kazuya Nagano [a,1], So-ichiro Kanasaki [a,b], Yuka Maeda [a,b], Takeshi Furuya [a,b], Masaki Inoue [a], Hiromi Nabeshi [b], Tomoaki Yoshikawa [a,b], Yasuo Yoshioka [a,b,c], Norio Itoh [b], Yasuhiro Abe [a], Haruhiko Kamada [a,c], Yasuo Tsutsumi [a,b,c], Shin-ichi Tsunoda [a,c,d,*]

[a] Laboratory of Biopharmaceutical Research, National Institute of Biomedical Innovation, 7-6-8 Saito-Asagi, Ibaraki, Osaka 567-0085, Japan
[b] Laboratory of Toxicology and Safety Science, Graduate School of Pharmaceutical Sciences, Osaka University, 1-6 Yamadaoka, Suita, Osaka 565-0871, Japan
[c] The Center for Advanced Medical Engineering and Informatics, Osaka University, 1-6 Yamadaoka, Suita, Osaka 565-0871, Japan
[d] Laboratory of Biomedical Innovation, Graduate School of Pharmaceutical Sciences, Osaka University, 1-6 Yamadaoka, Suita, Osaka 565-0871, Japan

ARTICLE INFO

Article history:
Received 27 March 2012
Available online 4 April 2012

Keywords:
Malignant mesothelioma
Cisplatin susceptibility
Annexin A4
Biomarker
Proteomics

ABSTRACT

Mesothelioma is a highly malignant tumor with a poor prognosis and limited treatment options. Although cisplatin (CDDP) is an effective anticancer drug, its response rate is only 20%. Therefore, discovery of biomarkers is desirable to distinguish the CDDP-susceptible versus resistant cases. To this end, differential proteome analysis was performed to distinguish between mesothelioma cells of different CDDP susceptibilities, and this revealed that expression of annexin A4 (ANXA4) protein was higher in CDDP-resistant cells than in CDDP-susceptible cells. Furthermore, ANXA4 expression levels were higher in human clinical malignant mesothelioma tissues than in benign mesothelioma and normal mesothelial tissues. Finally, increased susceptibility was observed following gene knockdown of ANXA4 in mesothelioma cells, whereas the opposite effect was observed following transfection of an ANXA4 plasmid. These results suggest that ANXA4 has a regulatory function related to the cisplatin susceptibility of mesothelioma cells and that it could be a biomarker for CDDP susceptibility in pathological diagnoses.

1. Introduction

Malignant mesothelioma is an aggressive neoplasm located on serosal membrane surfaces such as the pleura, and less frequently the peritoneum, and it has a poor outcome. The five-year survival rate is only about 5%. On the other hand, it is well known that asbestos is the major causative agent in the development of this disease [1–3]. Moreover, malignant mesothelioma takes 40–50 years to develop following exposure to asbestos. Because of its adiabatic potential, asbestos was commonly used as a building material in the 1960–1970s. Thus, an increase in mesothelioma patients is expected in the future. Patients with pleural malignant mesothelioma commonly present with an effusion associated with breathlessness that is often accompanied by chest-wall pain and a cough. After confirming the diagnosis, many patients are treated by intensive multidirectional approaches that combine cytoreductive surgery with intrapleural or intraperitoneal chemotherapy [4–8]. However, cytoreductive surgery is not always possible for patients with extensive intraperitoneal disease. Thus, the role of chemotherapy in malignant mesothelioma is critically important.

CDDP is an extensively used anticancer drug for the treatment of malignant mesothelioma, although the response rate is only about 20% [9–12]. A major problem with CDDP treatment of malignant mesothelioma patients is the development of CDDP insusceptibility. Thus, there is an urgent need to further our understanding of the pathogenesis of malignant mesothelioma, particularly with respect to the expression of proteins that confer drug susceptibility, in order to develop novel therapeutic strategies. In this study, a proteomic analysis was performed using high- and low-CDDP-susceptible malignant mesothelioma cells to identify candidate proteins associated with CDDP susceptibility.

2. Materials and methods

2.1. Cells

H28, H2052, H2452, H226 and MSTO-221H were purchased from American Type Culture Collection and maintained in RPMI1640 medium (Wako) containing 10% fetal calf serum (Biowest). Human mesothelial cells (HMC) were purchased from

* Corresponding author at: Laboratory of Biopharmaceutical Research, National Institute of Biomedical Innovation, 7-6-8 Saito-Asagi, Ibaraki, Osaka 567-0085, Japan. Fax: +81 72 641 9817.
E-mail address: tsunoda@nibio.go.jp (S.-i. Tsunoda).
[1] These authors contributed equally to this work.

0006-291X/$ - see front matter © 2012 Elsevier Inc. All rights reserved.
http://dx.doi.org/10.1016/j.bbrc.2012.03.144

Sciencell and cultured in Mesothelial Cell Growth Medium (ZenBio) under a 5% CO_2 atmosphere at 37 °C.

2.2. Measurement of cisplatin susceptibility in malignant mesothelioma cells

Malignant mesothelioma cells were seeded into 96-well microplates and cultured overnight. Various concentrations of CDDP were added to each well, the plates were incubated for 24 h, and cell viability was measured using Cell count reagent SF (Nacalai tesque). Absorbance was measured using a microplate reader (Bio-Rad) at test and reference wavelengths of 450 and 650 nm, respectively.

2.3. Proteomic analysis using two dimensional differential in-gel electrophoresis

For proteomic analysis, quantitative analysis was performed using two dimensional differential in-gel electrophoresis (2D-DIGE). Cell lysates were prepared from H28 and H2052 and then solubilized with 7 M urea, 2 M thiourea, 4% CHAPS and 10 mM Tris–HCl (pH 8.5). The lysates were labeled at the ratio of 50 μg proteins: 400 pmol Cy3 or Cy5 protein-labeling dye (GE Healthcare Biosciences) in dimethylformamide according to the manufacturer's protocol. The labelled samples were mixed with rehydration buffer (7 M urea, 2 M thiourea, 4% CHAPS, 2% DTT, 2% Pharmalyte (GE Healthcare Biosciences)) and applied to a 24-cm immobilized pH gradient gel strip (IPG-strip pH 4–7) for separation in the first dimension. For the second dimension separation, the IPG-strips were treated with iodoacetamide and applied to SDS–PAGE gels (10% polyacrylamide and 2.7% *N,N′*-diallyltartardiamide gels). After electrophoresis, the gels were scanned with a laser fluoroimager (Typhoon Trio, GE Healthcare Biosciences). The spot-picking gel was scanned after staining with Deep purple total protein stain (GE Healthcare Biosciences). Quantitative analysis of protein spots was carried out with Decyder-DIA software (GE Healthcare Biosciences). For the antigen spots of interest, spots of 1 mm × 1 mm in size were picked using Ettan Spot Picker (GE Healthcare Biosciences).

2.4. In-gel tryptic digestion

Picked gel pieces were destained with 50% acetonitrile/50 mM NH_4HCO_3 for 20 min twice, dehydrated with 75% acetonitrile for 20 min, and then dried using a centrifugal concentrator. Five microliter of 20 μg/ml trypsin (Promega) solution was added to each gel piece and the pieces were incubated for 16 h at 37 °C. The digested peptides were extracted sequentially using 50%, 80%, and 100% acetonitrile and then dried before being suspended in 10 μl of 0.1% formic acid.

2.5. Mass spectrometry and database search

Extracted peptides were analyzed by liquid chromatography ultra high resolution time-of-flight mass spectrometry (LC-UHR TOF-MS/MS; maXis, Bruker Daltonics). The Mascot search engine (http://www.matrixscience.com) was initially used to query the entire theoretical tryptic peptide database as well as SwissProt (http://www.expasy.org/, a public domain database provided by the Swiss Institute of Bioinformatics). The search query assumed the following: (i) the peptides were mono-, di- or tri-isotopic, (ii) methionine residues may be oxidized, (iii) all cysteines were modified with carbamidomethyl.

2.6. Western blot

The cell lysates were separated in 10% SDS–polyacrylamide gels and transferred to Immobilon membranes (Millipore). After blocking by 4% block ace (DS Pharma Biomedical) for 1 h at room temperature, the blots were reacted with primary antibodies in a buffer containing 0.4% block ace, and then with the appropriate peroxidase-conjugated secondary antibodies in the same buffer. Expression of ANXA4 in malignant mesothelioma cells was detected by mouse anti-human ANXA4 (Abnova: 1D3) followed by an HRP-conjugated anti-mouse IgG antibody (Sigma–Aldrich) using the ECL-plus system (GE Healthcare Biosciences). Equal amounts of protein loading were confirmed by parallel β-actin immunoblotting, and signal quantification was performed by densitometric scanning.

2.7. Immunohistochemistry staining

Human mesothelioma and normal tissue sections were deparaffinated in xylene and rehydrated in a graded series of ethanol dilutions. Heat-induced epitope retrieval was performed by incubating at different temperatures following the manufacturer's instructions using Target Retrieval Solution pH 9 (Dako). After heat-induced epitope retrieval treatment, endogenous peroxidase was blocked with a peroxidase blocking reagent (Dako). Following peroxidase blocking, the slides were incubated with 10% bovine serum albumin (BSA) solution for 30 min at room temperature. The slides were then incubated for 60 min with anti-human ANXA4 monoclonal antibody (9 μg/ml) in 3% BSA at room temperature. After washing 3 times with wash buffer (Dako), the slides were incubated for 30 min with ENVISION + Dual Link (Dako) at room temperature. They were then washed final 3 times and stained with 3,3′-diaminobenzidine. After development, the slides were lightly counterstained with Mayer's hematoxylin and mounted with resinous mounting medium.

2.8. Cisplatin susceptibility in cells transfected with ANXA4-siRNA and ANXA4-plasmid

H28 was transfected with ANXA4-siRNA (target sequence: AAGGATATCACAGAAGGATAT, Qiagen) using Hyperfect reagent (Qiagen) according to the manufacturer's instructions. In contrast, H2052 was transfected with ANXA4-pcDNA 3.1 (a gift from Naka T: Laboratory for Immune Signal, National Institute of Biomedical Innovation) using FuGENE HD transfection reagent (Roche). After transfection, the cells were treated with various concentrations of CDDP for 36 h (ANXA4-siRNA) or 24 h (ANXA4-pcDNA 3.1). Cell viability was measured as described above.

2.9. Statistical analysis

Differences in tumor volumes between the control and target groups were compared using the unpaired Student's *t*-test.

3. Results

3.1. CDDP susceptibility in malignant mesothelioma cells

Cell viability following CDDP treatment was examined to determine which cell lines had higher or lower susceptibility to CDDP. Among five tested mesothelioma cell lines, H2052 was the most and H28 the least susceptible cell line (Fig. 1). The IC_{50} values of H28, H2052, H2452, H226 and MSTO-221H were 154.5, 27.8, 66.0, 87.5 and 49.5 μM, respectively.